A bHLH interaction code controls bipotential differentiation and self-renewal in the *Drosophila* gut

Aleix Puig-Barbe[1,2], Svenja Dettmann[3,4], Vinicius Dias Nirello[5], Helen Moor[6], Sina Azami[7], Bruce A. Edgar[8,9], Patrick Varga-Weisz[5,6], Jerome Korzelius[7,8,11] and Joaquín de Navascués[1,6,✉]

[1] European Cancer Stem Cell Research Institute, School of Biosciences, Cardiff University, Hadyn Ellis Building, Maindy Road, Cardiff CF24 4HQ, UK.

[2] Current address: EMBL-European Bioinformatics Institute, Wellcome Genome Campus, Hinxton, Cambridgeshire, CB10 1SD, UK.

[3] DKFZ/ZMBH Alliance, University of Heidelberg, Heidelberg, Germany.

[4] AbbVie Germany GmbH & Co. KG, Frankfurt, Germany.

[5] International Laboratory for Microbiome Host Epigenetics, Department of Genetics, Evolution, Microbiology, and Immunology, Institute of Biology, University of Campinas, Campinas, SP 13083-862, Brazil

[6] School of Life Sciences, University of Essex, Wivenhoe Park, Colchester CO4 3SQ, UK.

[7] Max Planck Institute for Biology of Ageing, Joseph-Stelzmann-Straße 9B, 50931 Köln, Germany.

[8] DKFZ/ZMBH Alliance, University of Heidelberg, Heidelberg, Germany.

[9] Huntsman Cancer Institute & Dept. of Oncological Sciences, University of Utah, Salt Lake City, UT 84112, USA.

[11] School of Biosciences, University of Kent, Canterbury, Kent, CT2 7NZ, UK.

✉ j.denavascues@essex.ac.uk

Word count (Introduction to References): 6626

Running title: Da, Emc and Sc balance stemness and differentiation in the fly intestine

Key words: bHLH / stemness / differentiation / bipotent stem cell / intestinal stem cell

ABSTRACT (147)

Multipotent adult stem cells balance self-renewal with differentiation into various cell types. How this balance is regulated at the transcriptional level is poorly understood. Here we show that a network of basic Helix-Loop-Helix (bHLH) transcription factors controls both stemness and bi-potential differentiation in the *Drosophila* adult intestine. We find that homodimers of Daughterless (Da), homolog of mammalian E proteins, maintain self-renewal of intestinal stem cells (ISCs), antagonising the Enteroendocrine fate promoted by heterodimers of Da and Scute (Sc, homolog of ASCL). The HLH factor Extramacrochaetae (Emc, homologous to Id proteins) promotes absorptive differentiation by titrating Da and Sc. Emc prevents the committed absorptive progenitor from de-differentiating, underscoring the plasticity of these cells. Switching physical interaction partners in this way enables the active maintenance of stemness while priming stem cells for differentiation along two alternative fates. Such regulatory logic is likely operative in other bipotent stem cell systems.

INTRODUCTION

The regulation of stem cell fate decisions hinges on transcriptional control by sequence-specific transcription factors (TFs) forming gene regulatory networks that steer cells along particular differentiation trajectories (Graf and Enver, 2009; Levine and Davidson, 2005; Moris et al., 2016). These trajectories are often considered a succession of binary steps regulated by cross-antagonism between TF pairs (Graf and Enver, 2009; Simon et al., 2018). However, active multipotent stem cells need to decide between the maintenance of their stem identity and several options of commitment into distinct mature cell fates. To understand how multipotent stem cells make these choices, knowledge of the functional interactions between transcription factors is essential (Cinquin and Demongeot, 2005; 2002).

Intestinal stem cells (ISCs) are a paradigm of multipotency in adult tissues. ISCs face a choice between self-renewal and differentiation into either the secretory or absorptive cell lineage (reviewed in Crosnier et al., 2006; Jiang and Edgar, 2012; Philpott and Winton, 2014). The intestinal secretory lineage in *Drosophila* consists of enteroendocrine cells (EE) (Micchelli and Perrimon, 2006; Ohlstein and Spradling, 2006). Absorptive cells are called enterocytes (ECs) and differ in morphology and function along the anterior-posterior axis of the gut (Buchon et al., 2013; Marianes and Spradling, 2013). In *Drosophila*, ISCs produce lineage-specific precursors through distinct molecular triggers. High Notch signalling induces formation of enteroblasts (EBs), which will give rise to ECs. Expression in ISCs of the bHLH (basic Helix-Loop-Helix) transcription factors Scute (Sc) or Asense (Ase), members of the *achaete-scute Complex* (*AS-C*, homologs of *ASCL* mammalian genes) induces the formation of EE precursors (pre-EEs), which quickly turn into EE cells (Bardin et al., 2010; Chen et al., 2018; Zeng and Hou, 2015). It is not clear whether upon ISC division, daughter cells first commit to differentiation before choosing a lineage (two consecutive binary decisions), or are already lineage-primed before they lose self-renewing ability (binary decisions in inverse order), or choose at the same time between self-renewal and two potential lineages to commit to (single triple decision) (Gervais and Bardin, 2017; Perdigoto et al., 2011). Little is known about the molecular mechanisms that could allow a triple decision between self-renewal and bi-potential differentiation.

The bHLH family of transcription factors control cell fate in multiple developmental contexts (reviewed in Bertrand et al., 2002; Murre, 2005; Murre et al., 1994). Their HLH motif mediates dimerization, while the preceding region, rich in basic amino acids, allows DNA binding (reviewed in Massari and Murre, 2000). Class I of bHLH factors

comprises proteins such as E47, E2-2 and HEB (E proteins, encoded by *TCF3/4/12* in mammals; *daughterless —da—* in *Drosophila*). Class I bHLH proteins can make dimers within their class (e.g., Da:Da, or E47:HEB), but also heterodimerise with class II bHLH factors. By contrast, class II bHLH factors such as MYOD or ASCL (MyoD and proteins encoded in the *AS-C* in *Drosophila*) usually form trans-activating complexes only in heterodimers with class I factors (Murre et al., 1994). Both class I and class II factors can heterodimerise with class V proteins (reviewed in Campuzano, 2001; Wang and Baker, 2015). The mammalian members of this class are named *Inhibitors of DNA binding* (Id proteins) because they lack the stretch of basic amino acids preceding the HLH domain, rendering their heterodimers unable to bind DNA (Murre et al., 1994). Their only homolog in *Drosophila* is *extra macrochaetae* (*emc*).

Class II bHLH factors regulate differentiation in the metazoan intestine (reviewed in Hartenstein et al., 2017; Philpott and Winton, 2014). In *Drosophila*, Sc and Ase can initiate EE differentiation (Amcheslavsky et al., 2014; Bardin et al., 2010; Chen et al., 2018; Z. Guo and Ohlstein, 2015), while other bHLH factors maintain EE function (Dimmed, homolog of NeuroD; Beebe et al., 2015), or promote their functional diversity (Tap, homolog of Neurogenin-3; Hartenstein et al., 2017). On the other hand, Da is required for ISC maintenance, as ISCs mutant for *da* differentiate (Bardin et al., 2010; Lan et al., 2018). However, the interaction partners of Da to maintain stemness are not known, and how different bHLH factors dimerise to control differentiation has not been explored. Here we identify the Da homodimer as the critical bHLH complex maintaining ISC self-renewal and find a role of Emc in titrating Da and Sc to promote absorptive differentiation. We show that Da:Da and Da:Sc dimers functionally cooperate promoting ISC fate, but act antagonistically for EE differentiation. Our results reveal a network of bHLH factors that forms a three-way switch to regulate self-renewal and bipotential differentiation in the adult fly gut.

RESULTS

Da homodimers maintain stemness and prevent differentiation

We quantified the effect of *da* on differentiation in individual null da^{10} clones using the MARCM method (**Figure S1A-B**; Lee and Luo, 1999) and in the entire ISC/EB population by RNAi-mediated knock-down of *da* followed by lineage tracing using the *escargot* Flip-Out approach ("esg^{TS}-*FO*", see **Figure S1C**; Jiang et al., 2009). Loss of *da* led to almost complete differentiation of cells into ECs, and occasionally into EEs, in da^{10} mutant clones (**Figure 1A-B, I** and **Tables S1-2**) and in the esg^{+} cells expressing da^{RNAi} (**Figure 1C-E, I**; cell type markers as in **Figure S1D**). By contrast, in ISCs and EBs that overexpressed *da* with esg^{TS}-*FO*, differentiation into ECs was almost completely impaired, while EE differentiation increased (**Figure 1F, I**). Importantly, only a few esg^{+} cell nests overexpressing *da* survived and this was rescued by co-expression of apoptosis inhibitor p35 (**Figure 1J-K**). While the cell composition of esg^{TS}-*FO* > *da* tissue was very different to the wild type, the size of GFP^{+} clusters expressing *da* was like in the controls: most remained below 5 cells, and a few became considerably larger (**Figure 1L**).

We sought to determine the identity of the Da partners involved in preventing EC differentiation. Since Da can form homodimers to control differentiation and proliferation (reviewed in Wang and Baker, 2015), we overexpressed forced Da homodimers using a *da:da* tethered construct (Tanaka-Matakatsu et al., 2014) with esg^{TS}-*FO* to test their capacity to block differentiation. The resulting GFP^{+} tissue comprised mostly ISCs and EBs, which distributed in clusters of similar size to the wild type (**Figure 1G, I, L**). To test that Da homodimers were enough to maintain self-renewal without other Da-containing complexes, we expressed Da:Da while removing endogenous Da with the da^{RNAi} transgene *P{TRiP.JF02488}*, which does not target the *da:da* construct (**Figure S1E**). This prevented differentiation entirely (all cells were either ISCs or EBs; **Figure 1H-I**). In addition, we detected no esg^{+} cell death when the tethered *da:da* construct was overexpressed (**Figures 1G-H**, compare with **Figure 1J**). Together, these results show that Da homodimers promote stemness; additionally, Da probably participates in another complex that induces esg^{+} cell death.

Da:Sc and Da:Da antagonise each other in secretory differentiation

Our results so far indicate that EE differentiation requires the transition from the transcriptional program of Da:Da to that of Da:Sc. This could occur through a 'switch', with Da:Sc targets being epistatic over those of Da:Da, or 'antagonism', whereby the

111 relative strengths of the two programs determine cell fate. To distinguish between
112 these alternatives, we compared the effects of overexpressing *sc* with *esg*^{TS}*-FO* with
113 those of co-expressing *da* and *sc*. Overexpression of *sc* alone leads to the induction of
114 Pros-positive, Dl-negative and Dl/Pros double-positive cells (**Figures 2A and S2A**), as
115 expected (Bardin et al., 2010; Chen et al., 2018). This was likely mediated by Da:Sc,
116 as co-expression of *sc* and *da*^{RNAi} strongly diminished the induction of all Pros-positive
117 cells (**Figure S2A-C**). Many of these cells exhibited the mitotic marker phospho-
118 Histone H3S10 (PH3) (**Figure S2D**) and were probably trapped in a pre-EE state
119 (Chen et al., 2018). The co-expression of *da* and *sc* greatly reduced the number of
120 Pros-positive, Dl-negative (EE) cells and led to an increase in all Dl-positive cells
121 (**Figure 2B, D**), while maintaining mitotic figures (**Figure S2E, G**). Since endogenous
122 *da* is expressed weakly (Bardin et al., 2010), the overexpression of *da* and *sc* will likely
123 produce more Da:Sc dimers than that of *sc* alone. Therefore, the suppression of the *sc*
124 phenotype by *da+sc* must be due to a higher Da:Da-to-Da:Sc ratio. This suggests
125 antagonism between Da:Sc and Da:Da, and predicts that the co-expression of tethered
126 *da:da* and *sc* would result in even less EE differentiation, as endogenous Da available
127 for Da:Sc dimers will be limiting. Indeed, we observed a ~2-fold increase of Dl-positive,
128 Pros-negative cells at the expense of all Pros-positive cells, especially the Dl-negative
129 (**Figure 2C-D**), with an increase in PH3^{+} cells (**Figure S2F-G**).

130 Loss of Notch leads to formation of masses of Pros-positive, EE-like cells (Bardin et al.,
131 2010; Ohlstein and Spradling, 2006; **Figure 2E**). We further tested whether Da
132 homodimers antagonise EE differentiation by co-expressing *da:da* and *Notch*^{RNAi} with
133 *esg*^{TS}*-FO*, and found that Pros-positive appeared isolated and in low numbers (**Figure
134 2F**). Thus, Da:Da and Da:Sc oppose each other in EE differentiation; intriguingly, they
135 seem to collaborate to induce proliferation (**Figure S2D-G**) and the formation of Dl-
136 positive, Pros-negative ISCs (**Figure 2A-D**).

137 **Da:Da and Da:Sc collaborate to promote ISC identity**

138 To understand how Da:Da and Da:Sc activate antagonistic transcriptional programs,
139 we performed mRNA-seq analysis of purified *esg-Gal4 UAS-GFP* ISCs and EBs that
140 overexpressed either *da*^{RNAi}, *da*, *da:da* or *sc*. All conditions gave distinct transcriptional
141 signatures (**Figures 3A** and **S3A** and **Table S3**). Interestingly, ~1/3 of the genes
142 downregulated upon *da*^{RNAi} expression were common to those on *da* overexpression
143 (**Figure 3A**). To explore these transcriptional signatures further, we looked at 57 cell
144 type marker genes for ISCs, EBs, pECs and EEs (**Table S4**), and found that both loss
145 and gain of Da downregulate EE-specific genes (**Figures 3B** and **S3C**). This may

146 reflect that Da homodimers prevent EE differentiation (**Figures 1G-I** and **2B-D**) while
147 Da:Sc dimers induce it (Li et al., 2017; **Figure S2A-C**). Consistent with this,
148 overexpression of *sc* strongly induced EE-specific genes; it also increased expression
149 of the ISC-specific genes *spdo* and *Dl*. Overexpression of *da:da* or *da* alone induced
150 ISC-specific genes (*mira*, *spdo*), while most genes expressed in the absorptive lineage
151 (*myo31DF*, *nub/pdm1*, α*Try*, β*Try*; *E(spl)m*β*-HLH*, *E(spl)m3-HLH*, and other *E(spl)*
152 genes outside the 57-gene panel) were upregulated in da^{RNAi} overexpression and
153 downregulated in the other conditions (**Figures 3B** and **S3B-C**). Thus, the
154 transcriptome analysis supports our histofluorescence observations.

155 To determine whether the regulated genes were potential direct targets, we scored
156 predicted regulatory elements close to differentially expressed genes for transcription
157 factor binding motifs. We found E-boxes and other bHLH binding sites
158 over-represented in upregulated genes upon *da* or *da:da* overexpression and
159 downregulated ones upon da^{RNAi} overexpression (**Figure 3C** and **Table S5**).

160 Gene Set Enrichment Analysis (GSEA) showed that da^{RNAi} induced genes expressed in
161 the absorptive lineage while reducing the expression of ISC- and EE-specific genes.
162 Meanwhile, *sc* overexpression did the opposite, leading to stronger expression of ISC-
163 specific genes than *da:da* overexpression (**Figure 3D**). We looked at individual genes
164 within the regulated, ISC-specific genes. While overexpression of either *da:da* or *sc*
165 induced regulatory genes such as *Dl* or *mira*, they had opposite effects on genes
166 encoding factors involved in DNA replication (*Orc2*, *Mcm2*, *Mcm5*, *Mcm6* and *Mcm7*) or
167 mitosis (*polo*, *aurB*, *BubR1* and *Ncd80*): these were repressed by *da:da* but induced by
168 *sc* (**Figure 3E-F**). This highlights the capacity of *sc* to regulate key ISC-specific genes.

169 We also found differences in broad functional annotations between the overexpression
170 of da^{RNAi} and that of *da*, *da:da* or *sc*. While loss of Da induces genes involved in
171 metabolism, biosynthesis and energy storage and consumption, Da, Da:Da and Sc
172 reduced the expression signatures of these processes and favoured signalling and
173 regulatory genes (**Figure S3D-E**). We conclude that Da:Da and Da:Sc induce distinct
174 signatures that promote the ISC and EE identities, respectively, and repress the active
175 metabolism typical of EC function. However, Da:Da represses ISC-specific genes
176 involved in replication and mitosis, which are upregulated by Da:Sc.

177 Sc and Da can impart ISC properties

178 The transcriptional effects of *da:da* and *sc* overexpression on ISC-specific genes
179 prompted us to evaluate the capacity of *sc*, *da* or *da:da* to impose ISC properties on

more differentiated cells. We targeted EB, which are lineage-committed and postmitotic, using the driver *NRE^{TS}-FO* (**Figure S4A**). Wild-type EBs labelled with *NRE^{TS}-FO* either remained undifferentiated or became ECs; negligible numbers expressed Dl or Pros (**Figure 4A, E**). Driving expression of *sc*, *da* or *da:da* with *NRE^{TS}-FO* abolished EC differentiation and led to a significant increase of Dl-positive cells (**Figure 4B-E**). *sc* overexpression in EBs also induced many pre-EEs and EE cells (**Figure 4D-E**). This suggested that Da, Da:Da and Sc could force EBs to revert to the ISC fate and, in the case of Sc, also to the secretory lineage. We evaluated whether these Dl-positive cells could, like ISCs do, undergo mitosis. We found mitotic (PH3-positive) cells within the EB-derived Dl-positive cells overexpressing *sc*; their proportion was of the same order as the mitotic, endogenous ISCs within the same tissue (2% vs 7%; **Figure 4F-G**). To assess whether *sc* may be promoting ISC properties in normal homeostasis, we analysed published single-cell RNAseq (scRNAseq) datasets (Hung et al., 2020; Li et al., 2022) (**Figure S4B**), and found that cells classified as ISC/EBs that expressed *sc* had on average much higher levels of *Dl* (**Figure 4H**), suggesting that *sc*, apart from inducing EE differentiation, normally promotes expression of ISC features.

Emc promotes EC differentiation by titrating Da

Da and Sc functions are often antagonised through direct binding and titration by the HLH class V factor Emc, which prompted us to test *emc* function in intestinal homeostasis. Using the protein trap line *emc^{CPTI002740}* (Lowe et al., 2014), we found *emc* expressed in all cell types of the adult gut but predominantly by EBs and ECs (**Figures 5A-C**). scRNAseq data (Hung et al., 2020; Li et al., 2022) show that *emc* expression is mainly in EBs and ECs of the posterior midgut, with cell type distributions similar to bona-fide markers of posterior midgut ECs (pECs) and EBs (**Figure S5A-H**). Consistent with this, *emc* expression decreases along the transcriptional trajectory from ISC/EB to EE and increases in the ISC/EB to pEC trajectory (**Figures 5D** and **S5I**). MARCM clones mutant for *emc^{LL02590}* (**Figure S5J**) had fewer differentiated cells and were enriched in Dl-positive ISCs (**Figure 5E-F**, **J**). Clones for alleles *emc^{1}* and *emc^{AP6}* (**Figure S5J**) showed similar enrichment in Dl-positive ISCs compared to wild-type clones (**Figure 5G-J**). Hypomorphic viable *emc^{LL02590}/emc^{1}* and *emc^{LL02590}/emc^{P5C}* heterozygotes (**Figure S5J**) showed an increase in ISCs/EBs at the expense of ECs, accompanied by higher levels of Dl in ISCs and its ectopic expression in ECs, compared to control *emc^{LL02590}*/+ guts (**Figure 5K-N**). Knockdown of *emc* with *esg^{TS}-FO* phenocopied the overexpression of *da*: ISCs/EBs gave rise to labelled clusters of

215 similar size to the controls (**Figure 1L**) where differentiation was severely impaired
216 (**Figure 5O-Q, S**). The strength of the effect on differentiation in the *emc*^{RNAi} transgenes
217 correlated with their efficacy in depleting Emc protein and inducing *extra macrochaetae*
218 phenotypes (**Figure S5K-R**). The strongest *emc*^{RNAi} (*NIG-1007R*) induced, as with *da*
219 overexpression, the loss of many *esg*$^{+}$ cell nests by apoptosis (as death was prevented
220 by co-expression of p35; **Figure S6A-B**). We conclude that *emc* is necessary for EC
221 differentiation and the survival of ISCs and EBs. Overexpression of *emc* with *esg*^{TS}*-FO*
222 resulted in all ISCs/EBs differentiating into ECs (**Figure 5R-S**), as expected (Lan et al.,
223 2018). Therefore, Emc is both necessary and sufficient to direct absorptive
224 differentiation.

225 If Emc promoted EC differentiation by titrating Da and Sc, *emc* function should depend
226 on *da*. We tested this by generating MARCM clones mutant for *da* and expressing
227 *emc*^{RNAi} or mutant for *emc* and expressing *da*^{RNAi}. Both conditions led to EC
228 differentiation like in *da*^{10} clones (**Figure 6A-C**, compare with **6D**). Considering our
229 previous results where *sc* promoted ISC characteristics (**Figures 3** and **4**) and that
230 ISCs express Sc (Chen et al., 2018; Doupé et al., 2018), we tested whether the effects
231 of *emc* loss depended on *sc* or any other member of the *AS-C*. We induced MARCM
232 clones for *Df(1)sc*^{B57} (a deletion of the *AS-C*; González et al., 1989) expressing *emc*^{RNAi}
233 and compared them with clones that only expressed *emc*^{RNAi}. Differentiation was
234 impaired in both conditions (**Figure 6F-G**), but Dl expression was four-fold lower in the
235 absence of the AS-C (**Figure 6H**). We conclude that Emc promotes EC differentiation
236 and dampens Dl expression by preventing formation of Da:Da and Da:Sc dimers,
237 respectively.

238 ***emc* is required for the commitment of EBs**

239 The requirement of *emc* for differentiation prompted us to investigate whether it was
240 necessary to maintain the commitment of EBs as absorptive progenitors. We used the
241 EB-specific driver *NRE*^{TS}*-Gal4*, which never co-expresses with Dl in the wild-type, to
242 express *emc*^{RNAi}. This led to Dl expression in *NRE*$^{+}$ cells (**Figure S6C-D**), suggesting
243 that *emc*-depleted EBs may revert to ISCs. We verified this with *NRE*^{TS}*-FO* driving
244 *emc*^{RNAi} expression and observed that *emc*-depleted EBs give raise to Delta-positive
245 cells (**Figure 6I-J**) that undergo mitosis (PH3-positive) at similar frequency to
246 neighbouring normal ISCs (**Figure 6I, K**). This suggests that *emc* is necessary for the
247 commitment of EBs.

248 **Da/Emc regulate ISC date independently of Notch**

249 Notch signalling is key for ISC differentiation and absorptive fate acquisition (Micchelli
250 and Perrimon, 2006; Ohlstein and Spradling, 2006). We found that simultaneous
251 knock-down of *N* and *da* with *esg*^{TS}*-FO* prevented the tumorous expansion of
252 Dl-positive and Pros-positive cells typically found with *N*^{RNAi} alone (Micchelli and
253 Perrimon, 2006; Patel et al., 2015) and led to ECs differentiation (**Figure S7A-B**). This
254 suggests that Notch could be regulating *da*. To activate or prevent Notch signalling, we
255 used *esg*^{TS}*-FO* to knock-down or overexpress Hairless (H), the specific co-repressor
256 for the transcriptional targets of Notch (reviewed in Bray and Furriols, 2001).
257 Overexpression of *H* with *esg*^{TS}*-FO* resulted in expansion of Dl-positive cells and EE
258 differentiation (**Figure 7A, I**; Bardin et al., 2010). Simultaneously knocking down *da*
259 significantly induces EC differentiation, but not to the levels induced by *da* knock-down
260 alone (**Figure 7B, I**). Conversely, expression of *H*^{RNAi} with *esg*^{TS}*-FO* leads to an
261 increase in EC differentiation (**Figure 7C**; Bardin et al., 2010) and the expression of
262 *NRE-lacZ* in all diploid cells (**Figure 7I**). The co-expression of *da:da* with *H*^{RNAi} prevents
263 all EC differentiation, but extends *NRE-lacZ* expression to all *esg*$^{+}$ cells, at the expense
264 of Dl (**Figure 7D, I**). Thus, simultaneously inducing or interfering with *da* and Notch
265 signalling leads to phenotypes in between their respective individual manipulations.
266 This suggests that *da* and Notch signalling can act in parallel.

267 *emc* transcription is regulated by Notch signalling in other tissues (Adam and Montell,
268 2004; Baonza et al., 2000; Baonza and Freeman, 2001; Bhattacharya and Baker,
269 2009; Spratford and Kumar, 2015), and we found that co-expressing *emc* and *N*^{RNAi}
270 with *esg*^{TS}*-FO* leads to EC differentiation (**Figure S7C**). Therefore, it is possible Notch
271 could induce EC differentiation at least partially through *emc*. We found that *emc*
272 expression induces EC differentiation rapidly (Puig-Barbe, 2018), so these
273 *esg*^{TS}*-FO>emc+N*^{RNAi} ECs could have differentiated before N protein was depleted. To
274 inhibit Notch signalling faster, we co-expressed *emc* and *H* with *esg*^{TS}*-FO*. This led to
275 an increase in EC differentiation compared to expression of *H* alone, but far from the
276 near-complete EC differentiation observed when only expressing *emc* (**Figure S7D-G**).
277 This suggests that Emc can induce differentiation in the absence of Notch signalling,
278 but not efficiently. Moreover, expressing *H*^{RNAi} and *emc*^{RNAi} with *esg*^{TS}*-FO* did not
279 prevent the excess EC differentiation observed upon expression of *H*^{RNAi} alone; this
280 contrasts with the capacity of *emc*^{RNAi} to block differentiation entirely (**Figure S7D, H-**
281 **J**). Therefore, Emc is dispensable for Notch to induce EC differentiation. Moreover,
282 clonal expression of the Notch intracellular domain does not induce *emc* expression in
283 any cell type of the midgut epithelium (**Figure S7K**). We conclude that *emc* and Notch
284 signalling act independently to promote the absorptive fate.

285 **Da:Da and Esg block differentiation independently**

286 Esg, a transcription factor of the Snail family, regulates ISCs by preventing ISC/EB
287 differentiation (Korzelius et al., 2014; Loza-Coll et al., 2014). As Da:Da dimers have the
288 same capacity, we considered whether Esg and Da act together to maintain stemness.
289 Expression of *esg*^{RNAi} with *esg*^{TS}*-FO* led to differentiation into ECs and EEs (**Figure 7E,**
290 **J**), as expected (Korzelius et al., 2014; Li et al., 2017; Loza-Coll et al., 2014).
291 Simultaneous overexpression of *esg*^{RNAi} and *da:da* blocked EC differentiation and
292 significantly reduced formation of EEs (**Figure 7F, J**). In turn, expression of *esg* with
293 *esg*^{TS}*-FO* blocked differentiation, irrespective of whether *da*^{RNAi} was also expressed
294 (**Figure 7G-H, J**). This independence seems mirrored in their down-regulated gene
295 sets: almost half the Esg repression targets overlap with genes downregulated by
296 misexpression of *da* or *da:da* or upregulated by misexpression of *da*^{RNAi}, including
297 genes essential for EC function like *nub/pdm1*, *ssk* and *Tsp2A* (**Figure 7K**). Finally, we
298 observed that expression of neither *da* nor *esg* were affected by the overexpression
299 the other (**Figure S7L-M**). We conclude that *da* and *esg* contribute to stemness
300 independently of each other.

301

302 **DISCUSSION**

303 We demonstrate a central role for a bHLH factor code in the acquisition and
304 maintenance of three alternative cell fates in the adult *Drosophila* intestine. Class I
305 homodimers (Da:Da) maintain the progenitor state of ISCs/EB, with changes in
306 dimerization partners governing the fate transitions. Sequestration of Da with class V
307 HLH factor Emc into Da:Emc dimers incapable of DNA binding induces progenitor cells
308 to acquire the absorptive fate, while formation of Da:Sc dimers by binding of Da with
309 class II bHLH Sc initiates EE differentiation (**Figures 2** and **S2**; Bardin et al., 2010;
310 Zeng and Hou, 2015). Moreover, Emc is required in EBs to maintain their committed
311 state, while low levels of Sc boost aspects of the ISC transcriptional state.

312 **Three cell fates regulated by a dimerization network**

313 Networks involving class I, II and V bHLH factors regulate the development of the
314 *Drosophila* retina (Bhattacharya and Baker, 2011) and peripheral nervous system
315 (Cubas et al., 1991; Troost et al., 2015; Van Doren et al., 1991). However, in these
316 cases, the choice is between only two alternative fates (neural vs epidermal), with Da
317 homodimers promoting the same fate as heterodimers between Da and a class II
318 bHLH proneural factor (Bhattacharya and Baker, 2011; Li and Baker, 2018; Troost et
319 al., 2015). By contrast, in the adult midgut Da:Da and Da:Sc promote distinct fates
320 (progenitor and secretory, respectively) through distinct transcriptional programs while
321 Emc titrates both dimers to allow EC differentiation. This integrated mechanism
322 suggests that the balance between ISC self-renewal and absorptive or secretory
323 differentiation rests on a triple choice, rather than two consecutive binary decisions. An
324 equivalent network could operate in similar stem cell systems, and it is tempting to
325 speculate of this possibility in the mammalian intestine, where the relevant factors
326 (mouse *da* homologs *E2a* and *Heb*, *emc* homolog *Id1* and *sc* homolog *Acsl1*) are
327 expressed in the crypts of Lieberkühn and have roles in fate determination (van der
328 Flier et al., 2009; Wice, 1998; Zhang et al., 2014).

329 **A balance of factors regulates intestinal stem cell fate**

330 We refer to the Da/Emc/Sc network as a bHLH 'code' due to its modularity, but it does
331 not behave as a Boolean switch; the relative abundance of the different components
332 seems critical. Da, the centrepiece of the network, forms homodimers that maintain
333 stemness and prevent EC and EE differentiation (**Figures 1** and **2**), but it is also an
334 essential partner for Sc in EE differentiation (**Figure S2**). The activity of Da
335 homodimers in promoting stemness is also nuanced, as in parallel to activating some

336 ISC genes and repressing some EE/EC ones, Da:Da downregulates proliferation
337 effector proteins, in agreement with its previously reported anti-proliferative activity
338 (Andrade-Zapata and Baonza, 2014). Strikingly, an excess of Da monomers (whether
339 induced by direct overexpression or indirectly by loss of Emc) promotes apoptosis
340 (**Figures 1** and **S6**), while the excess of Sc or tethered Da:Da does not. It follows that
341 Da also participates in an apoptosis-promoting complex yet to be identified. By
342 contrast, the activity of Emc is determinant, but not intrinsically instructive: through
343 titration of Da and Sc cells have to differentiate but lack the capacity to initiate EE
344 differentiation, so they differentiate into ECs by default. However, Emc loss in EBs
345 induces expression of ISC features, possibly through the increased activity of Sc
346 (**Figure 6**), and prevents Da from inducing apoptosis of ISC/EBs (**Figure S6**). This
347 makes Emc also an essential factor to maintain the progenitor population. Sc, which is
348 normally expressed at low levels in ISCs (Chen et al., 2018; Doupé et al., 2018),
349 triggers EE differentiation when expressed over a threshold (Amcheslavsky et al.,
350 2014; Bardin et al., 2010; Chen et al., 2018). We find that Sc boosts expression of
351 essential ISC genes, such as Dl or those involved in proliferation. Moreover, Sc seems
352 to induce fate reversal in EBs. Therefore, Sc also boosts the ISC function, which sits
353 well with the role of its homolog *Acsl2* in maintaining mammalian ISCs (van der Flier et
354 al., 2009).

355 We conclude that a dynamic balance of Da, Emc and Sc is required for homeostasis,
356 and this bHLH code is not composed not of 'master' but contextual regulators. This
357 pushes the question towards the regulation of their protein concentrations and/or
358 functions across intestinal cell types and over time.

359 In line with this view, other essential regulators of ISC fate operate in parallel to the
360 bHLH network. Excess of either Esg or Da can compensate for the absence of each
361 other to maintain ISCs/EBs undifferentiated, suggesting that at physiological levels,
362 when either is essential for stemness (**Figure 1**; Korzelius et al., 2014), they have
363 some additive effect. This may be reflected in the significant overlap of their
364 downregulated genes (**Figure 7**), which includes the EC-fate inducer *nub/pdm1*. On
365 the other hand, Esg seems to have a more specific role than Da:Da in preventing EE
366 differentiation and lacks its anti-proliferative activity (Korzelius et al., 2014; Loza-Coll et
367 al., 2014), suggesting that they also govern non-shared aspects of ISC identity and
368 function. Similarly, both Notch signalling and Emc can induce EC differentiation in the
369 absence of the other, which suggests that the absorptive fate does not simply arise by

370 default when Da and Sc are not functioning. These multiple, non-redundant layers of
371 regulation likely allow fine-tuning the ISC function.

372 **Multiple factors maintain enteroblast commitment**

373 Notch signalling induces the formation of EBs (Micchelli and Perrimon, 2006; Ohlstein
374 and Spradling, 2006), which under normal conditions give rise to mature ECs without
375 further division (Wang et al., 2015; Yin and Xi, 2018; Zeng and Hou, 2015; **Figure 4**).
376 EBs are relatively long-lived (Antonello et al., 2015), and though they are recognised
377 by expression of the *NRE*, once formed they do not need Notch to maintain their
378 commitment (Siudeja et al., 2015). However, we found that they require Emc, as its
379 depletion in EBs gave rise to Dl-expressing proliferative cells–likely a reversal of fate
380 towards ISC. Qualitatively similar effects resulted from mis-expressing *da*, *da:da* or *sc*
381 in EBs. We interpret that combined baseline levels of Da and Sc in EBs may lead them
382 to revert their fate into ISCs if not titrated by Emc. EB-to-ISC reversion is also
383 prevented by transcription factor Sox21a (Zhai et al., 2015) and the global co-repressor
384 Groucho (Guo et al., 2019). EB-to-EE trans-differentiation has also been observed,
385 when Ttk69 or Klu were depleted, or Phyllopod overexpressed, in EBs (Korzelius et al.,
386 2019; Wang et al., 2015; Yin and Xi, 2018). These observations underscore the
387 plasticity of the EB and resemble the behaviour of EC precursors in the mammalian
388 intestine, which can dedifferentiate and repopulate the intestinal crypt during
389 regeneration (Tetteh et al., 2016).

390 **Limitations of the study**

391 Our interpretation of the functional relationships between Da, Sc and Emc are based
392 on misexpression tools with no control over resulting stoichiometry. Future studies
393 should address this limitation with newly developed tools with more precise control
394 (Goldner et al., 2023; Yesbolatova et al., 2020; Diao and White, 2012). Our analysis of
395 *emc* function involved the emc^{RNAi} transgene *NIG-1007R*, which is far more effective at
396 depleting Emc than either *KK108316* or *JF02300* or both combined (**Figure S5**).
397 Several *emc* loss of function conditions affecting large amounts of tissue induce
398 increased Dl expression (**Figure 5**), but with *NIG-1007R* this effect is much higher and
399 not observed in MARCM *emc* null clones. This may point to non-cell-autonomous,
400 suppressing effects on Dl expression that are only inactivated when the whole tissue or
401 the whole progenitor population are affected. We are confident that *NIG-1007R* elicits
402 genuine *emc* loss phenotypes, because the strength of the increase in Dl levels
403 correlates with the strength of the emc^{RNAi} transgenes (**Figures 5** and **S6**); *NIG-1007R*

404 phenocopies the overexpression of *da*, including the induction of apoptosis (which
405 *KK108316* and *JF02300* cannot recapitulate; **Figures 1**, **5** and **S5**); we can fully rescue
406 the increase in Dl expression induced by *NIG-1007R* by simultaneous loss of *sc*
407 (**Figure 6**). While our tenet does not hinge on this observation, it deserves future
408 attention.

409

ACKNOWLEDGEMENTS

We thank the anonymous reviewers for helpful suggestions, Nicholas Baker, Allison Bardin, Antonio Baonza, Sonsoles Campuzano, Sangbin Park, Mike Taylor, Shinya Yamamoto, Alfonso Martínez-Arias, the Bloomington *Drosophila* Stock Center, the Vienna *Drosophila* Resource Center, the *Drosophila* Genetics Resource Center (Kyoto) and the National Institute of Genetics (Japan) for providing fly stocks, the Developmental Studies Hybridoma Bank (University of Iowa) for supplying antibodies, and Juan Modolell, Sonsoles Campuzano, Catherine Hogan, Fernando dos Anjos-Afonso, Florian Siebzehnrubl, Terrence Trinca, Sonia López de Quinto, Helen White-Cooper, Mike Taylor and Wynand van der Goers van Naters for critical comments on the manuscript and useful discussions. We acknowledge the data analysis team of the College of Biomedical and Life Sciences of Cardiff University and the FACS and Imaging Core Facility at the Max Planck Institute for Biology of Ageing for technical assistance.

This work was supported by funding from Cardiff University to JdN and AP, from the University of Essex and NC3Rs SKT grant NC/W001047/1 to PVW and JdN, a DFG-Grant KO5594/1-1 and an EMBO Long-Term Fellowship to JK, a FAPESP fellowship #2021/00393-9 to VDN, a FAPESP São Paulo Excellence Chair #2019/16113-5 to PVW, and an ERC Advanced Grant no. 268515 to BAE.

JdN dedicates this work to the memory of Juan Modolell and Rosa María Aguilar.

AUTHOR CONTRIBUTIONS

Conception of study, supervision: JdN. Data acquisition: AP, SD, SA, JK, HM and JdN. Analysis and interpretation: AP, VDN, JdN, JK. Training, supervision: JdN, JK, PVW, BE. Writing the manuscript: JdN, AP. Revising and approval of the manuscript: all authors.

CONFLICT OF INTEREST

The authors declare no competing interest.

438 **FIGURE LEGENDS**

439 **Figure 1. Da homodimers are required and sufficient to maintain ISCs**
440 **undifferentiated.**
441 **A-B.** Cells in MARCM clones for *da*^{10} (B) are mostly ECs. ISCs, EBs and EEs are
442 dramatically reduced respect to wild-type clones (A). Panel B is reproduced in **Figure**
443 **6A** to aid comparison. **C-E.** Expressing *da*^{RNAi} with *esg*^{TS}*-FO* using transgenes
444 *JF02488* (D) and *HMS01851* (E) leads to the differentiation of most cells into ECs,
445 occasionally into EEs. Controls (C) maintain ISCs and EBs. Solid and empty
446 arrowheads (A-E): ECs and ISCs or EEs, respectively. **F-G.** Overexpression of *da* (F)
447 or *da:da* (G) with *esg*^{TS}*-FO* prevents formation of ECs; *da* overexpression allows EE
448 differentiation and strongly reduces *esg*$^{+}$ cell nest density. Solid arrowheads (F-G):
449 ISCs/EBs. **H.** Overexpression of *da:da* with *esg*^{TS}*-FO* while depleting endogenous Da
450 with *JF02488* interferes blocks all differentiation. **I.** Cell composition of GFP^{+} tissue and
451 clones from A-H. Some data are reproduced in **Figure 7I-J** to aid comparison. **J-K.**
452 Expression of *da* with *esg*^{TS}*-FO* (J) results in *esg*$^{+}$ cell death, with few survivors that
453 cannot differentiate; co-expression of *p35* (K) rescues cell death, but not differentiation.
454 J is a wider field of view than the tissue shown in panel F. Arrows: *esg*$^{+}$ Hdc^{+} ISCs/EBs.
455 **L.** Histograms of GFP^{+} cluster sizes for *esg*^{TS}*-FO* driving expression of *da*, *da:da*,
456 *emc*^{RNAi} and their control. The X axis is truncated at 16 cells, but there were larger
457 clusters in all conditions except *emc*^{RNAi}, at frequencies of 0.3% or lower. DAI: days
458 after induction. Scale bars: 20μm. *p*-values (binomial regression for individual cell
459 types): ● < 0.05; ●● < 0.01; ●●● < 0.001. See **Tables S1-2** for statistical details.
460

461 **Figure 2. Da:Sc and Da:Da antagonise each other in EE differentiation.**
462 **A-C.** Overexpression of *sc* with *esg*^{TS}*-FO* leads to a dramatic increase of pre-EEs and
463 EEs, but maintains a population of ISCs (A). The ISC fraction progressively increases
464 by co-expression of *da* (B) and tethered *da:da* (C), at the cost of EE differentiation (B,
465 C) and pre-EE formation (C). **D.** Cell composition of GFP^{+} tissue from A-C. **E-F.** Knock-
466 down of *Notch* with *esg*^{TS}*-FO* results in excess of EEs and ISCs (E); simultaneous
467 overexpression of *da:da* rescues both phenotypes (F). Solid and empty arrowheads:
468 pre-EEs and ISCs, respectively; asterisks: EEs. Panel E is reproduced in **Figure S7A**
469 to aid comparison. DAI: days after induction. Scale bars: 20μm. *p*-values (binomial
470 regression): ● < 0.05; ●● < 0.01; ●●● < 0.001. See **Tables S1-2** for statistical details.
471

472 **Figure 3. Da and Sc cooperate to induce the ISC transcriptional signature.**

473 **A.** Euler diagram with the sizes of gene sets differentially expressed
474 (at $|\log_2(FC)| \geq 1.5$), and their approximate intersections, upon *da*^{RNAi}, *da:da*, *da* and *sc*
475 overexpression. **B.** MA plots for *esg*^{TS} > *sc*, *da:da*, *da* and *da*^{RNAi}, respectively. Cell type
476 markers are shown in colours matching **Figure 1I**. **C**. Normalised enrichment scores
477 (NES) of DNA motifs found in differentially expressed genes ($|\log_2(FC)| \geq 1.5$) in the
478 four conditions analysed. Dots represent individual motifs, coloured by the transcription
479 factor family that binds them. Some swarms show their bHLH motif fraction. **D**. NES
480 heatmap for cell-type specific gene sets; coloured asterisks indicate significance. **E-F.**
481 Enrichment plots of the transcriptional profiles induced by *sc* (E) or *da:da* (F) for ISC-
482 and EE-specific genes. *sc* induces a clear EE signature. Some ISC genes involved in
483 replication (*Orc2*, *Mcm2*, *5*, *6* and *7*) and mitosis (*BubR1*, *polo*, *aurB*, *sti*, *Ndc80*) are
484 repressed by *da:da* but activated by *sc*.
485
486 **Figure 4. Da:Sc and Da:Da can impose ISC properties on EBs.**
487 **A-D.** Expression of either *da* (B), *da:da* (C) or *sc* (D) with *NRE*^{TS}*-FO* (see **Figure S4A**)
488 blocks normal EC differentiation (compare with A) and promotes re-expression of Dl
489 (empty arrowheads) and EE differentiation (solid arrowheads). EB-derived EEs occur
490 occasionally upon *da* or *da:da* overexpression but are very frequent upon *sc*
491 overexpression, which also induces the formation of pre-EEs. **E.** Cell composition of
492 GFP$^+$ tissue from A-D. **F.** Overexpression of *sc* with *NRE*^{TS}*-FO* shows both Dl$^+$ and
493 Pros$^+$ cells (empty and solid arrowheads, respectively) undergoing mitosis (phospho-
494 H3$^+$). **G.** Proportions of mitotic Dl$^+$ cells (Pros$^+$ or Pros$^-$) within and out of the
495 population of cells co-expressing *GFP* and *sc* in *NRE*^{TS}*-FO>GFP* + *sc* intestines
496 (N=303 cells). **H.** Expression of *Dl* found in ISCs/EBs by scRNAseq (see **Figure S4B**),
497 segregated by the expression of *scute* (zero vs non-zero counts). DAI: days after
498 induction. Scale bars: 20µm. *p*-values (binomial regression): ● < 0.05; ●● < 0.01; ●●●
499 < 0.001. See **Tables S1-2** for statistical details.
500
501 **Figure 5. *emc* is necessary and sufficient to induce EC differentiation.**
502 **A-C.** Expression of Emc-GFP in the homozygous viable protein-trap insertion
503 *emc*^{CPTI002740}. Emc is expressed in EBs (*NRE-lacZ*$^+$, arrowheads) (A) and some ECs
504 (*myoIA-lacZ*$^+$, solid arrowheads) but not all (empty arrowheads) (B). Some ISCs (Dl$^+$,
505 solid arrowheads) and EEs (Pros$^+$, solid asterisks) express Emc, but many do not
506 (empty arrowheads and asterisks) (C). **D.** *emc* expression along the pseudotime
507 trajectories from ISC/EB cells into EEs and ECs (**Figure S5I**) decreases towards the
508 secretory fate and increases towards the absorptive one. **E-I.** Cells in MARCM clones
509 for *emc*^{LL02590} (F), *emc*^{AP6} (H) and *emc*^{1} (I) are enriched in ISCs (solid arrowheads) and

510 EBs (empty arrowheads) compared to controls (E and G). *FRT*$_{80B}$ and *FRT*$_{2A}$ are two
511 independent insertions for inducing MARCM clones in chromosomal arm 3L. **J.** Cell
512 composition of clones from E-I. **K-M.** Midguts of viable hypomorphic mutants
513 *emc*$^{LL02590/1}$ (L) and *emc*$^{LL02590/P5C}$ (M) contain more ISCs, preEEs (L, asterisk) and EEs,
514 and less ECs, than heterozygous controls (K). In these mutants, Dl expression is
515 elevated in some ISCs (L, M, empty arrowheads) and ectopic in some ECs (L, M, solid
516 arrowheads). **N.** Cell composition in genotypes from K-M. **O-Q.** Expressing *emc*^{RNAi}
517 with *esg*^{TS}*-FO* using transgenes *NIG-1007R* (P) or *KK108316* and *JF02300* together
518 (Q) increases the proportion of Dl^{+} cells and EEs (empty arrowheads) and reduces that
519 of ECs (solid arrowheads) compared to controls (O). *emc*^{RNAi} also increases Dl
520 expression (P, Q), especially with *NIG-1007R* (P). **R.** Overexpression of *emc* with
521 *esg*^{TS}*-FO* forces differentiation into ECs. **S.** Cell composition in genotypes from O-R.
522 DAI: days after induction. Scale bars: 20μm. *p*-values (binomial regression): ● < 0.05;
523 ●● < 0.01; ●●● < 0.001. See **Tables S1-2** for statistical details. Panels F, P, R are
524 reproduced in **Figures 6D, S7J, G**, respectively, to aid comparison.
525
526 **Figure 6. *emc* antagonises *da* and *sc* in the intestine and maintains EBs**
527 **committed.**
528 **A-D.** *da* is epistatic over *emc*. Solid arrowheads: ECs; empty arrowheads: ISCs. Cells
529 in MARCM clones that are mutant for *da*^{10} and express *emc*^{RNAi} *NIG-1007R* (B) mostly
530 differentiate into ECs, like in *da*^{10} clones (A). Cells in MARCM clones that are mutant
531 for *emc*^{LL02590} and express *da*^{RNAi} *JF02488* (C) also differentiate into ECs, suppressing
532 the reduced differentiation of *emc*^{LL02590} cells (D). **E.** Cell composition of clones from A-
533 D and **Figure 1I**. Note that *da*^{10} is statistically indistinguishable from *da*^{10}; *emc*^{RNAi}. **F-G.**
534 Emc antagonises Sc in inducing *Dl*. Loss of the *achaete/scute-Complex* (*AS-C*) using
535 deficiency *Df(1)sc*^{B57} reduces the elevated Dl expression observed with *emc*^{RNAi} (G,
536 compare with F). **H.** Quantification of relative levels of Dl per cell, normalised by Pros
537 (see Methods), for 210, 146, 718 and 210 cells per group from left to right. Horizontal
538 lines are averages per category. *p*-values (Mann-Whitney test): ✳✳✳ < 0.001; n.s., ≥
539 0.05. **I-K.** Expressing *emc*^{RNAi} *NIG-1007R* with *NRE*^{TS}*-FO* prevents EB differentiation
540 and activates Dl expression (I', solid arrowheads) at higher levels than extant ISCs
541 (arrowheads; extant ISCs are detectable after contrast-limited adaptive histogram
542 equalization, CLAHE). These cells are mitotic (I'', phospho-Histone H3, asterisks) at
543 levels similar to extant ISCs (K) and have presumably reverted into ISCs (quantified in
544 J). Scale bars: 20μm. *p*-values (binomial regression in stacked bars): ● < 0.05; ●● <
545 0.01; ●●● < 0.001; n.s. ≥ 0.05. See **Tables S1-2** for statistical details. Panels A, D are
546 reproduced from **Figures 1B, 5F**, respectively, to aid comparison.

547

548 **Figure 7. *da* is epistatic to Notch signalling and acts in parallel with *esg*.**
549 **A-B.** Expressing *H* with *esg*^{TS}*-FO* (A) blocks EC differentiation and leads to
550 accumulation of ISCs. This is rescued by simultaneous expression of *da*^{RNAi} (B). Solid
551 arrowheads: ISCs; empty arowheads: EEs. **C-D**. Expressing *H*^{RNAi} with *esg*^{TS}*-FO* (C)
552 induces EC differentiation, some EE differentiation (asterisk) and the expression of the
553 *NRE-lacZ* reporter in all *esg*$^{+}$ cells (solid arrowhead). Simultaneous expression of *da:da*
554 (D) blocks the formation of ECs, as in *esg*^{TS}*-FO>da:da* alone, and all cells become
555 *NRE-lacZ*$^{+}$ (solid arrowheads). **E-F.** Knock-down of *esg* with *esg*^{TS}*-FO* (E) induces
556 differentiation of all cells into ECs and EEs (solid arrowheads); this is prevented by
557 simultaneous expression of *da:da* (F), which blocks differentiation of ISCs (empty
558 arrowheads) and EBs (solid arrowheads) to the same levels as in *esg*^{TS}*-FO>da:da*
559 alone. **G-H.** Expression of *esg* with *esg*^{TS}*-FO* (G) blocks differentiation regardless of
560 whether *da* is simultaneously knocked-down (H). Empty arrowheads: ISCs; solid
561 arrowheads: EBs. DAI: days after induction. Scale bars: 20μm. **I-J.** Cell composition of
562 GFP^{+} tissue from A-D and E-H, respectively; data from **Figure 1I** is replicated here to
563 aid comparison. *p*-values (binomial regression for individual cell types): ● < 0.05; ●● <
564 0.01; ●●● < 0.001. See **Tables S1-2** for statistical details. **K.** Modified Euler diagram
565 showing the overlap between gene sets repressed directly by Esg (white) with those
566 either repressed by overexpression of *da* (blue) or *da:da* (yellow) or de-repressed by
567 expression of *da*^{RNAi} (red), all three at $|\log_2(FC)| \geq 1$). Areas approximate set sizes and
568 their intersections. Overlaps between *da*-regulated sets are not depicted. *p*-values for
569 overlap sizes (Esg∩Da, Esg∩Da:Da and Esg∩*da*^{RNAi}; hypergeometric test with
570 Bonferroni correction) are: ∗∗∗ < 1e–36, ∗ < 0.01, ∗ < 0.05.

571

572 **REFERENCES**

573 Adam, J.C., Montell, D.J., 2004. A role for extra macrochaetae downstream of Notch in
574 follicle cell differentiation. Development 131, 5971–5980. doi:10.1242/dev.01442
575 Amcheslavsky, A., Song, W., Li, Q., Nie, Y., Bragatto, I., Ferrandon, D., Perrimon, N.,
576 Ip, Y.T., 2014. Enteroendocrine Cells Support Intestinal Stem-Cell- Mediated
577 Homeostasis in Drosophila. CellReports 1–19. doi:10.1016/j.celrep.2014.08.052
578 Andrade-Zapata, I., Baonza, A., 2014. The bHLH Factors Extramacrochaetae and
579 Daughterless Control Cell Cycle in Drosophila Imaginal Discs through the
580 Transcriptional Regulation of the cdc25 Phosphatase string. PLoS Genet 10,
581 e1004233–16. doi:10.1371/journal.pgen.1004233
582 Antonello, Z.A., Reiff, T., Ballesta-Illan, E., Dominguez, M., 2015. Robust intestinal
583 homeostasis relies on cellular plasticity in enteroblasts mediated by miR-8-
584 Escargot switch. EMBO J. doi:10.15252/embj.201591517
585 Baonza, A., de Celis, J.F., Garcia-Bellido, A., 2000. Relationships between
586 extramacrochaetae and Notch signalling in Drosophila wing development.
587 Development 127, 2383–2393.
588 Baonza, A., Freeman, M., 2001. Notch signalling and the initiation of neural
589 development in the Drosophila eye. Development 128, 3889–3898.
590 Bardin, A.J., Perdigoto, C.N., Southall, T.D., Brand, A.H., Schweisguth, F., 2010.
591 Transcriptional control of stem cell maintenance in the Drosophila intestine.
592 Development 137, 705–714. doi:10.1242/dev.039404
593 Beebe, K., Park, D., Taghert, P.H., Micchelli, C.A., 2015. The Drosophila Prosecretory
594 Transcription Factor dimmed Is Dynamically Regulated in Adult Enteroendocrine
595 Cells and Protects Against Gram-Negative Infection. G3 (Bethesda) 5, 1517–1524.
596 doi:10.1534/g3.115.019117
597 Bertrand, N., Castro, D.S., Guillemot, F., 2002. Proneural genes and the specification
598 of neural cell types. Nat Rev Neurosci 3, 517–530. doi:10.1038/nrn874
599 Bhattacharya, A., Baker, N.E., 2011. A Network of Broadly Expressed HLH Genes
600 Regulates Tissue-Specific Cell Fates. Cell 147, 881–892.
601 doi:10.1016/j.cell.2011.08.055
602 Bhattacharya, A., Baker, N.E., 2009. Developmental Biology. Developmental Biology
603 327, 288–300. doi:10.1016/j.ydbio.2008.11.037
604 Bray, S., Furriols, M., 2001. Notch pathway: Making sense of suppressor of hairless.
605 Curr Biol 11, R217–R221. doi:10.1016/S0960-9822(01)00109-9
606 Buchon, N., OSMAN, D., David, F.P.A., Fang, H.Y., Boquete, J.-P., Deplancke, B.,
607 Lemaitre, B., 2013. Morphological and molecular characterization of adult midgut
608 compartmentalization in Drosophila. CellReports 3, 1725–1738.
609 doi:10.1016/j.celrep.2013.04.001
610 Campuzano, S., 2001. Emc, a negative HLH regulator with multiple functions in
611 Drosophila development. Oncogene 20, 8299–8307. doi:10.1038/sj.onc.1205162
612 Chen, J., Xu, N., Wang, C., Huang, P., Huang, H., Jin, Z., Yu, Z., Cai, T., Jiao, R., Xi,
613 R., 2018. Transient Scute activation via a self-stimulatory loop directs
614 enteroendocrine cell pair specification from self-renewing intestinal stem cells.
615 Nature Cell Biology 20, 152–161. doi:10.1038/s41556-017-0020-0
616 Cinquin, O., Demongeot, J., 2005. High-dimensional switches and the modelling of
617 cellular differentiation. J Theor Biol 233, 391–411. doi:10.1016/j.jtbi.2004.10.027
618 Cinquin, O., Demongeot, J., 2002. Positive and negative feedback: Striking a balance
619 between necessary antagonists. J Theor Biol 216, 229–241.
620 doi:10.1006/jtbi.2002.2544
621 Crosnier, C., Stamataki, D., Lewis, J., 2006. Organizing cell renewal in the intestine:
622 stem cells, signals and combinatorial control. Nat. Rev. Genet. 7, 349–359.
623 doi:10.1038/nrg1840

Cubas, P., de Celis, J.F., Campuzano, S., Modolell, J., 1991. Proneural clusters of achaete-scute expression and the generation of sensory organs in the Drosophila imaginal wing disc. Genes & Development 5, 996–1008.
Diao, F., White, B.H., 2012. A Novel Approach for Directing Transgene Expression in Drosophila: T2A-Gal4 In-Frame Fusion. Genetics 190, 1139–1144.
Doupé, D.P., Marshall, O.J., Dayton, H., Brand, A.H., Perrimon, N., 2018. Drosophila intestinal stem and progenitor cells are major sources and regulators of homeostatic niche signals. Proceedings of the National Academy of Sciences 115, 12218–12223. doi:10.1073/pnas.1719169115
Gervais, L., Bardin, A.J., 2017. Tissue homeostasis and aging: new insight from the fly intestine. Curr Opin Cell Biol 48, 97–105. doi:10.1016/j.ceb.2017.06.005
Goldner, A.N., Fessehaye, S.M., Rodriguez, N., Mapes, K.A., Osterfield, M., Doubrovinski, K., 2023. Evidence that tissue recoil in the early Drosophila embryo is a passive not active process. Mol. Biol. Cell 34, br16. doi:10.1091/mbc.E22-09-0409
González, F., Romani, S., Cubas, P., Modolell, J., Campuzano, S., 1989. Molecular analysis of the asense gene, a member of the achaete-scute complex of Drosophila melanogaster, and its novel role in optic lobe development. EMBO J 8, 3553–3562. doi:10.1002/j.1460-2075.1989.tb08527.x
Graf, T., Enver, T., 2009. Forcing cells to change lineages 462, 587–594. doi:10.1038/nature08533
Guo, X., Huang, H., Yang, Z., Cai, T., Xi, R., 2019. Division of Labor: Roles of Groucho and CtBP in Notch-Mediated Lateral Inhibition that Controls Intestinal Stem Cell Differentiation in Drosophila. Stem Cell Reports 1–26. doi:10.1016/j.stemcr.2019.03.005
Guo, Z., Ohlstein, B., 2015. Bidirectional Notch signaling regulates Drosophila intestinal stem cell multipotency. science (New York, NY) 350, aab0988–aab0988. doi:10.1126/science.aab0988
Hartenstein, V., Takashima, S., Hartenstein, P., Asanad, S., Asanad, K., 2017. bHLH proneural genes as cell fate determinants of entero-endocrine cells, an evolutionarily conserved lineage sharing a common root with sensory neurons. Developmental Biology 431, 36–47. doi:10.1016/j.ydbio.2017.07.013
Hung, R.-J., Hu, Y., Kirchner, R., Liu, Y., Xu, C., Comjean, A., Tattikota, S.G., Li, F., Song, W., Ho Sui, S., Perrimon, N., 2020. A cell atlas of the adult Drosophila midgut. Proceedings of the National Academy of Sciences 117, 1514–1523. doi:10.1073/pnas.1916820117
Jiang, H., Edgar, B.A., 2012. Intestinal stem cell function in Drosophila and mice. Curr. Opin. Genet. Dev. 1–7. doi:10.1016/j.gde.2012.04.002
Jiang, H., Patel, P.H., Kohlmaier, A., Grenley, M.O., McEwen, D.G., Edgar, B.A., 2009. Cytokine/Jak/Stat signaling mediates regeneration and homeostasis in the Drosophila midgut. Cell 137, 1343–1355. doi:10.1016/j.cell.2009.05.014
Korzelius, J., Azami, S., Ronnen-Oron, T., Koch, P., Baldauf, M., Meier, E., Rodriguez-Fernandez, I.A., Groth, M., Sousa-Victor, P., Jasper, H., 2019. The WT1-like transcription factor Klumpfuss maintains lineage commitment of enterocyte progenitors in the Drosophila intestine. Nat Commun 10, 4123–13. doi:10.1038/s41467-019-12003-0
Korzelius, J., Naumann, S.K., Loza-Coll, M.A., Chan, J.S., Dutta, D., Oberheim, J., Gläßer, C., Southall, T.D., Brand, A.H., Jones, D.L., Edgar, B.A., 2014. Escargot maintains stemness and suppresses differentiation in Drosophila intestinal stem cells. EMBO J 33, 2967–2982. doi:10.15252/embj.201489072
Lan, Q., Cao, M., Kollipara, R.K., Rosa, J.B., Kittler, R., Jiang, H., 2018. FoxA transcription factor Fork head maintains the intestinal stem/progenitor cell identities in Drosophila. Developmental Biology 433, 324–343. doi:10.1016/j.ydbio.2017.09.002

Lee, T., Luo, L., 1999. Mosaic analysis with a repressible cell marker for studies of gene function in neuronal morphogenesis. Neuron 22, 451–461.

Levine, M., Davidson, E.H., 2005. Gene regulatory networks for development. Proc Natl Acad Sci USA 102, 4936–4942. doi:10.1073/pnas.0408031102

Li, H., Janssens, J., De Waegeneer, M., Kolluru, S.S., Davie, K., Gardeux, V., Saelens, W., David, F.P.A., Brbić, M., Spanier, K., Leskovec, J., McLaughlin, C.N., Xie, Q., Jones, R.C., Brueckner, K., Shim, J., Tattikota, S.G., Schnorrer, F., Rust, K., Nystul, T.G., Carvalho-Santos, Z., Ribeiro, C., Pal, S., Mahadevaraju, S., Przytycka, T.M., Allen, A.M., Goodwin, S.F., Berry, C.W., Fuller, M.T., White-Cooper, H., Matunis, E.L., DiNardo, S., Galenza, A., O'Brien, L.E., Dow, J.A.T., FCA Consortium§, Jasper, H., Oliver, B., Perrimon, N., Deplancke, B., Quake, S.R., Luo, L., Aerts, S., Agarwal, D., Ahmed-Braimah, Y., Arbeitman, M., Ariss, M.M., Augsburger, J., Ayush, K., Baker, C.C., Banisch, T., Birker, K., Bodmer, R., Bolival, B., Brantley, S.E., Brill, J.A., Brown, N.C., Buehner, N.A., Cai, X.T., Cardoso-Figueiredo, R., Casares, F., Chang, A., Clandinin, T.R., Crasta, S., Desplan, C., Detweiler, A.M., Dhakan, D.B., Donà, E., Engert, S., Floc'hlay, S., George, N., González-Segarra, A.J., Groves, A.K., Gumbin, S., Guo, Y., Harris, D.E., Heifetz, Y., Holtz, S.L., Horns, F., Hudry, B., Hung, R.-J., Jan, Y.N., Jaszczak, J.S., Jefferis, G.S.X.E., Karkanias, J., Karr, T.L., Katheder, N.S., Kezos, J., Kim, A.A., Kim, S.K., Kockel, L., Konstantinides, N., Kornberg, T.B., Krause, H.M., Labott, A.T., Laturney, M., Lehmann, R., Leinwand, S., Li, J., Li, J.S.S., Li, K., Li, K., Li, L., Li, T., Litovchenko, M., Liu, H.-H., Liu, Y., Lu, T.-C., Manning, J., Mase, A., Matera-Vatnick, M., Matias, N.R., McDonough-Goldstein, C.E., McGeever, A., McLachlan, A.D., Moreno-Roman, P., Neff, N., Neville, M., Ngo, S., Nielsen, T., O'Brien, C.E., Osumi-Sutherland, D., Özel, M.N., Papatheodorou, I., Petkovic, M., Pilgrim, C., Pisco, A.O., Reisenman, C., Sanders, E.N., Santos, Dos, G., Scott, K., Sherlekar, A., Shiu, P., Sims, D., Sit, R.V., Slaidina, M., Smith, H.E., Sterne, G., Su, Y.-H., Sutton, D., Tamayo, M., Tan, M., Tastekin, I., Treiber, C., Vacek, D., Vogler, G., Waddell, S., Wang, W., Wilson, R.I., Wolfner, M.F., Wong, Y.-C.E., Xie, A., Xu, J., Yamamoto, S., Yan, J., Yao, Z., Yoda, K., Zhu, R., Zinzen, R.P., 2022. Fly Cell Atlas: A single-nucleus transcriptomic atlas of the adult fruit fly. science (New York, NY) 375, eabk2432. doi:10.1126/science.abk2432

Li, K., Baker, N.E., 2018. Regulation of the Drosophila ID protein Extra macrochaetae by proneural dimerization partners. eLife 7. doi:10.7554/eLife.33967

Li, Y., Pang, Z., Huang, H., Wang, C., Cai, T., Xi, R., 2017. Transcription Factor Antagonism Controls Enteroendocrine Cell Specification from Intestinal Stem Cells. Sci Rep 7, 988. doi:10.1038/s41598-017-01138-z

Lowe, N., Rees, J.S., Roote, J., Ryder, E., Armean, I.M., Johnson, G., Drummond, E., Spriggs, H., Drummond, J., Magbanua, J.P., Naylor, H., Sanson, B., Bastock, R., Huelsmann, S., Trovisco, V., Landgraf, M., Knowles-Barley, S., Armstrong, J.D., White-Cooper, H., Hansen, C., Phillips, R.G., UK Drosophila Protein Trap Screening Consortium, Lilley, K.S., Russell, S., St Johnston, D., 2014. Analysis of the expression patterns, subcellular localisations and interaction partners of Drosophila proteins using a pigP protein trap library. Development 141, 3994–4005. doi:10.1242/dev.111054

Loza-Coll, M.A., Southall, T.D., Sandall, S.L., Brand, A.H., Jones, D.L., 2014. Regulation of Drosophila intestinal stem cell maintenance and differentiation by the transcription factor Escargot. EMBO J 33, 2983–2996. doi:10.15252/embj.201489050

Marianes, A., Spradling, A.C., 2013. Author response. eLife 2, 155–19. doi:10.7554/eLife.00886

Massari, M.E., Murre, C., 2000. Helix-loop-helix proteins: regulators of transcription in eucaryotic organisms. Molecular and Cellular Biology 20, 429–440.

Micchelli, C.A., Perrimon, N., 2006. Evidence that stem cells reside in the adult Drosophila midgut epithelium. 439, 475–479. doi:10.1038/nature04371

733 Moris, N., Pina, C., Arias, A.M., 2016. Transition states and cell fate decisions in
734 epigenetic landscapes. Nat. Rev. Genet. 17, 693–703. doi:10.1038/nrg.2016.98
735 Murre, C., 2005. Helix-loop-helix proteins and lymphocyte development. Nat Immunol
736 6, 1079–1086. doi:10.1038/ni1260
737 Murre, C., Bain, G., VANDIJK, M.A., Engel, I., Furnari, B.A., Massari, M.E., Matthews,
738 J.R., Quong, M.W., Rivera, R.R., Stuiver, M.H., 1994. Structure and Function of
739 Helix-Loop-Helix Proteins. Biochim Biophys Acta 1218, 129–135.
740 doi:10.1016/0167-4781(94)90001-9
741 Ohlstein, B., Spradling, A., 2006. The adult Drosophila posterior midgut is maintained
742 by pluripotent stem cells. 439, 470–474. doi:10.1038/nature04333
743 Patel, P.H., Dutta, D., Edgar, B.A., 2015. Niche appropriation by Drosophila intestinal
744 stem cell tumours. Nature Cell Biology 17, 1182–1192. doi:10.1038/ncb3214
745 Perdigoto, C.N., Schweisguth, F., Bardin, A.J., 2011. Distinct levels of Notch activity for
746 commitment and terminal differentiation of stem cells in the adult fly intestine.
747 Development 138, 4585–4595. doi:10.1242/dev.065292
748 Philpott, A., Winton, D.J., 2014. Lineage selection and plasticity in the intestinal crypt.
749 Curr Opin Cell Biol 31, 39–45. doi:10.1016/j.ceb.2014.07.002
750 Puig-Barbé, A., 2018. A network of bHLH factors controls self-renewal and bipotential
751 differentiation in the Drosophila intestine. PhD thesis. Cardiff University.
752 Simon, C.S., Hadjantonakis, A.-K., Schröter, C., 2018. Making lineage decisions with
753 biological noise: Lessons from the early mouse embryo. WIREs Dev Biol 7, e319–
754 16. doi:10.1002/wdev.319
755 Siudeja, K., Nassari, S., Gervais, L., Skorski, P., Lameiras, S., Stolfa, D., Zande, M.,
756 Bernard, V., Frio, T.R., Bardin, A.J., 2015. Frequent Somatic Mutation in Adult
757 Intestinal Stem Cells Drives Neoplasia and Genetic Mosaicism during Aging. Cell
758 Stem Cell 17, 663–674. doi:10.1016/j.stem.2015.09.016
759 Spratford, C.M., Kumar, J.P., 2015. Inhibition of Daughterless by Extramacrochaetae
760 mediates Notch-induced cell proliferation. Development 142, 2058–2068.
761 doi:10.1242/dev.121855
762 Tanaka-Matakatsu, M., Miller, J., Borger, D., Tang, W.-J., Du, W., 2014. Daughterless
763 homodimer synergizes with Eyeless to induce Atonal expression and retinal neuron
764 differentiation. Developmental Biology 392, 256–265.
765 doi:10.1016/j.ydbio.2014.05.019
766 Tetteh, P.W., Basak, O., Farin, H.F., Wiebrands, K., Kretzschmar, K., Begthel, H., van
767 den Born, M., Korving, J., de Sauvage, F., van Es, J.H., van Oudenaarden, A.,
768 Clevers, H., 2016. Replacement of Lost Lgr5-Positive Stem Cells through Plasticity
769 of Their Enterocyte-Lineage Daughters. Cell Stem Cell 18, 203–213.
770 doi:10.1016/j.stem.2016.01.001
771 Troost, T., Schneider, M., Klein, T., 2015. A re-examination of the selection of the
772 sensory organ precursor of the bristle sensilla of Drosophila melanogaster. PLoS
773 Genet 11, e1004911. doi:10.1371/journal.pgen.1004911
774 van der Flier, L.G., van Gijn, M.E., Hatzis, P., Kujala, P., Haegebarth, A., Stange, D.E.,
775 Begthel, H., van den Born, M., Guryev, V., Oving, I., van Es, J.H., Barker, N.,
776 Peters, P.J., van de Wetering, M., Clevers, H., 2009. Transcription factor achaete
777 scute-like 2 controls intestinal stem cell fate. Cell 136, 903–912.
778 doi:10.1016/j.cell.2009.01.031
779 Van Doren, M., Ellis, H.M., Posakony, J.W., 1991. The Drosophila extramacrochaetae
780 protein antagonizes sequence-specific DNA binding by daughterless/achaete-scute
781 protein complexes. Development 113, 245–255.
782 Wang, C., Guo, X., Dou, K., Chen, H., Xi, R., 2015. Ttk69 acts as a master repressor of
783 enteroendocrine cell specification in Drosophila intestinal stem cell lineages.
784 Development 142, 3321–3331. doi:10.1242/dev.123208
785 Wang, L.-H., Baker, N.E., 2015. E Proteins and ID Proteins: Helix-Loop-Helix Partners
786 in Development and Disease. Dev Cell 35, 269–280.
787 doi:10.1016/j.devcel.2015.10.019

Wice, B.M., 1998. Forced Expression of Id-1 in the Adult Mouse Small Intestinal Epithelium Is Associated with Development of Adenomas. Journal of Biological Chemistry 273, 25310–25319. doi:10.1074/jbc.273.39.25310

Yesbolatova, A., Saito, Y., Kitamoto, N., Makino-Itou, H., Ajima, R., Nakano, R., Nakaoka, H., Fukui, K., Gamo, K., Tominari, Y., Takeuchi, H., Saga, Y., Hayashi, K.-I., Kanemaki, M.T., 2020. The auxin-inducible degron 2 technology provides sharp degradation control in yeast, mammalian cells, and mice. Nat Commun 1–13. doi:10.1038/s41467-020-19532-z

Yin, C., Xi, R., 2018. A Phyllopod-Mediated Feedback Loop Promotes Intestinal Stem Cell Enteroendocrine Commitment in Drosophila. Stem Cell Reports 10, 43–57. doi:10.1016/j.stemcr.2017.11.014

Zeng, X., Hou, S.X., 2015. Enteroendocrine cells are generated from stem cells through a distinct progenitor in the adult Drosophila posterior midgut. Development 142, 644–653. doi:10.1242/dev.113357

Zhai, Z., Kondo, S., Ha, N., Boquete, J.-P., Brunner, M., Ueda, R., Lemaitre, B., 2015. Accumulation of differentiating intestinal stem cell progenies drives tumorigenesis. Nat Commun 6, 10219–27. doi:10.1038/ncomms10219

Zhang, N., Yantiss, R.K., Nam, H.-S., Chin, Y., Zhou, X.K., Scherl, E.J., Bosworth, B.P., Subbaramaiah, K., Dannenberg, A.J., Benezra, R., 2014. ID1 Is a Functional Marker for Intestinal Stem and Progenitor Cells Required for Normal Response to Injury. Stem Cell Reports 3, 716–724. doi:10.1016/j.stemcr.2014.09.012

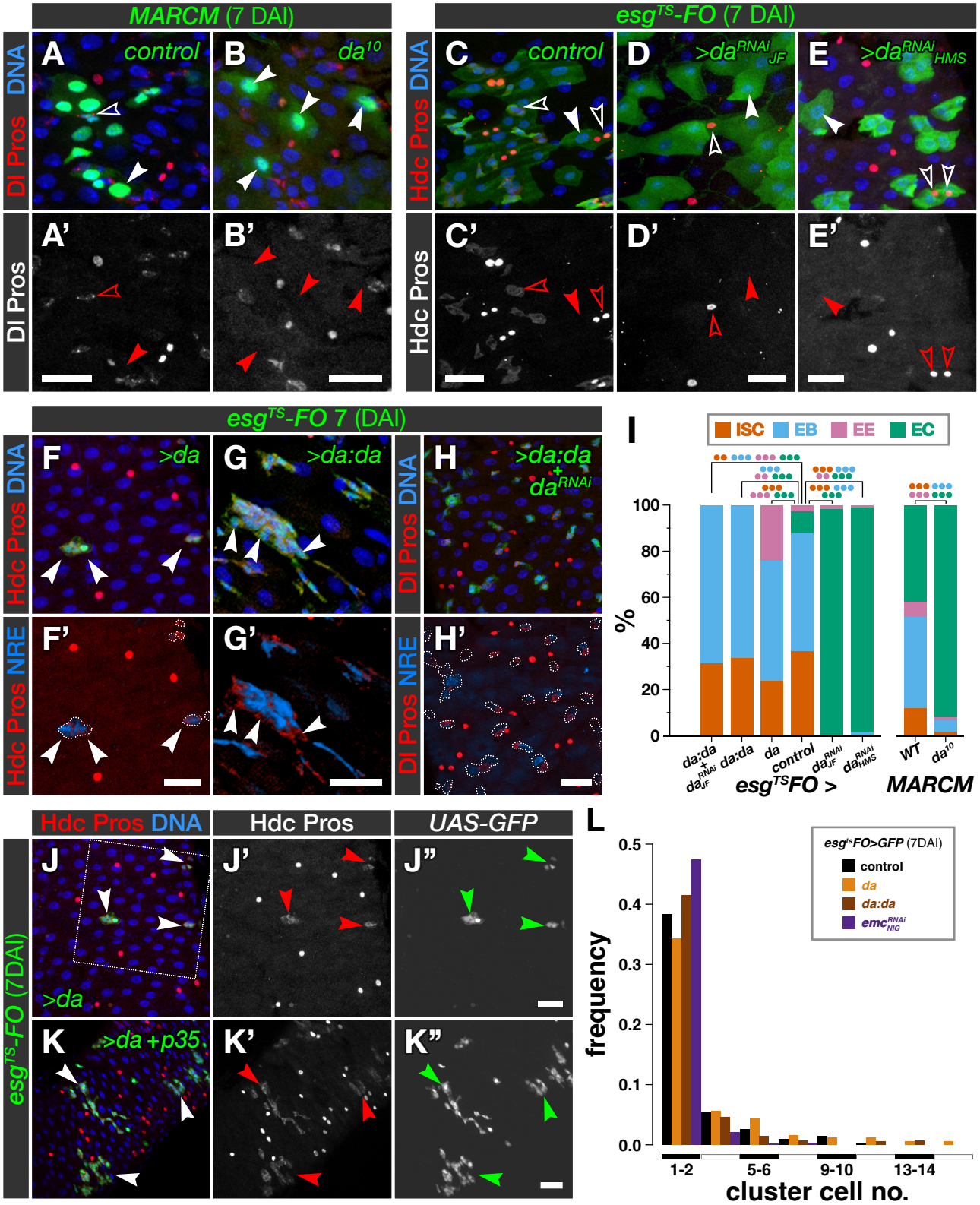
MARCM (7 DAI)
esgTS-FO (7 DAI)
DNA
Dl Pros
Hdc Pros
A control
B da10
C control
D >daRNAi JF
E >daRNAi HMS
A'
B'
C'
D'
E'
esgTS-FO 7 (DAI)
F >da
G >da:da
H >da:da + daRNAi
Hdc Pros NRE
Dl Pros NRE
F'
G'
H'
I
ISC
EB
EE
EC
%
100
80
60
40
20
0
da:da + daRNAi JF
da:da
da
control
daRNAi JF
daRNAi HMS
WT
da10
esgTSFO >
MARCM
Hdc Pros DNA
Hdc Pros
UAS-GFP
J
J'
J"
>da
esgTS-FO (7DAI)
K >da +p35
K'
K"
L
esgtsFO>GFP (7DAI)
control
da
da:da
emcRNAi NIG
frequency
0.5
0.4
0.3
0.2
0.1
0.0
1-2
5-6
9-10
13-14
cluster cell no.

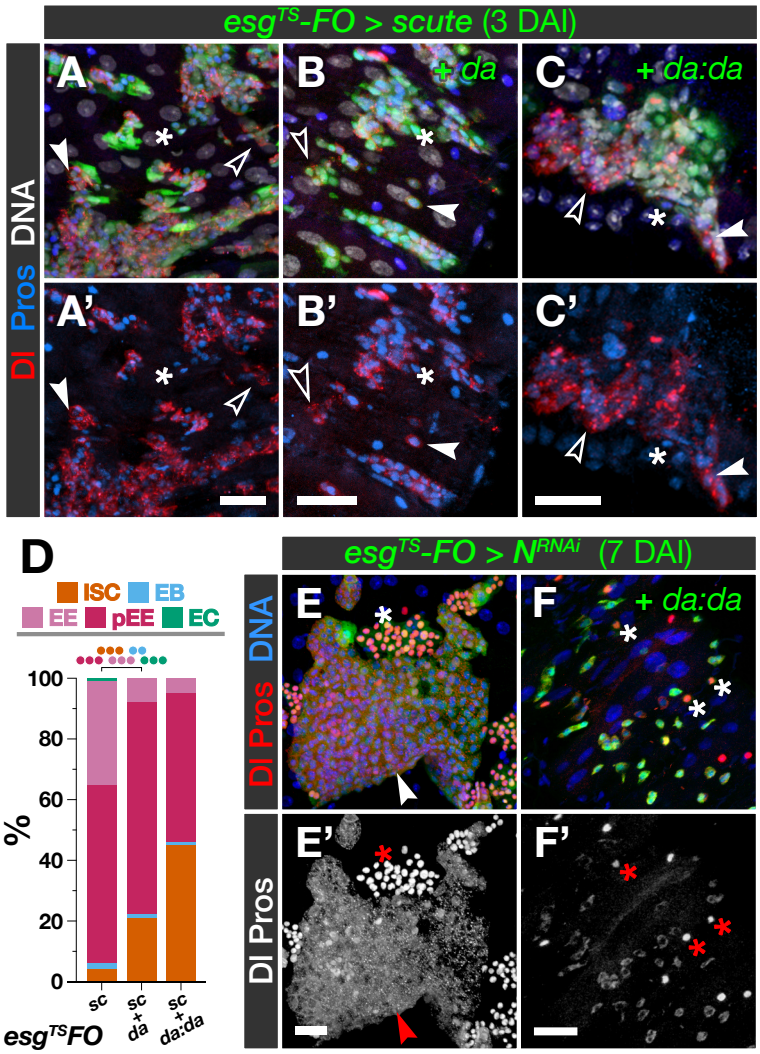
esgTS-FO > scute (3 DAI)
A
B
+ da
C
+ da:da
A'
B'
C'
DNA
Pros
Dl
D
ISC
EB
EE
pEE
EC
100
80
60
40
20
0
%
sc
sc + da
sc + da:da
esgTSFO
esgTS-FO > NRNAi (7 DAI)
E
F
+ da:da
E'
F'
DNA
Dl Pros
Dl Pros

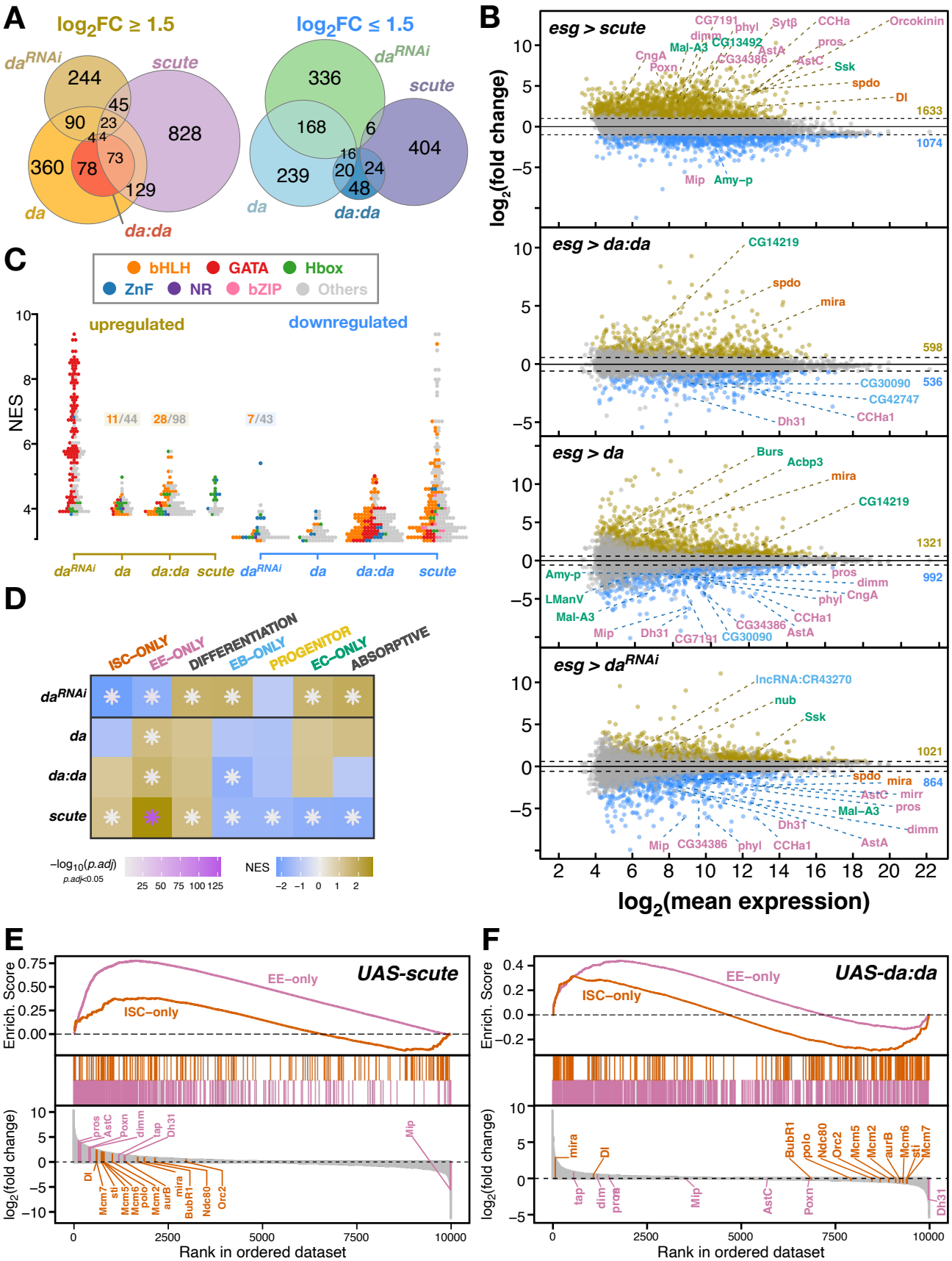
A
log2FC ≥ 1.5
daRNAi
scute
244
45
90
23
4 4
828
360
78
73
129
da
da:da
log2FC ≤ 1.5
daRNAi
scute
336
168
6
404
16
239
20
24
48
da
da:da
B
esg > scute
esg > da:da
esg > da
esg > daRNAi
log2(fold change)
log2(mean expression)
1633
1074
598
536
1321
992
1021
864
C
bHLH
GATA
Hbox
ZnF
NR
bZIP
Others
upregulated
downregulated
NES
11/44
28/98
7/43
daRNAi
da
da:da
scute
D
ISC–ONLY
EE–ONLY
DIFFERENTIATION
EB–ONLY
PROGENITOR
EC–ONLY
ABSORPTIVE
daRNAi
da
da:da
scute
–log10(p.adj)
p.adj<0.05
NES
E
UAS-scute
EE–only
ISC–only
Enrich. Score
log2(fold change)
Rank in ordered dataset
F
UAS-da:da
EE–only
ISC–only
Enrich. Score
log2(fold change)
Rank in ordered dataset

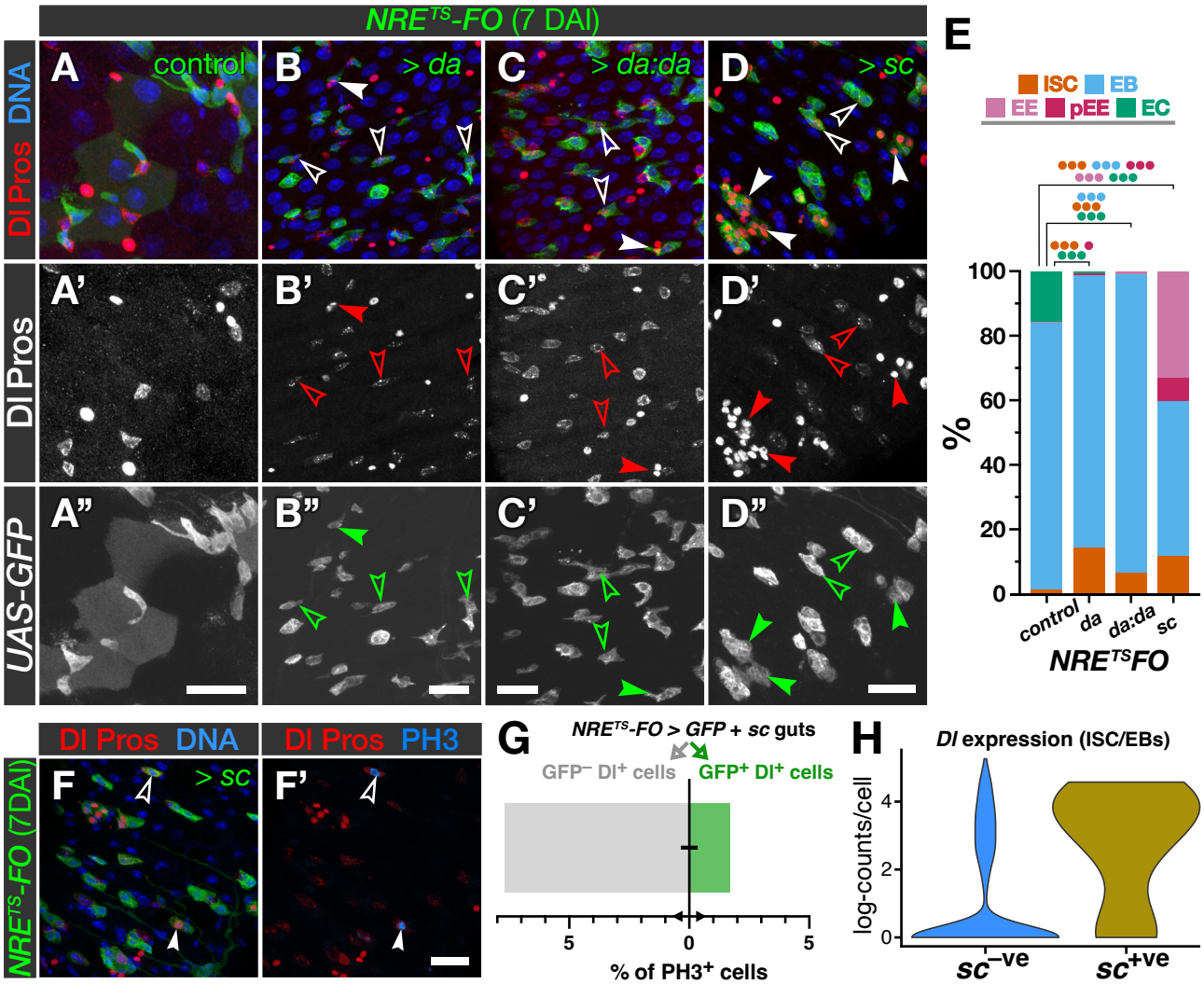
NRE^TS-FO (7 DAI)
Dl Pros DNA
Dl Pros
UAS-GFP
A control
B > da
C > da:da
D > sc
A'
B'
C'
D'
A"
B"
C'
D"
E
ISC EB
EE pEE EC
100
80
60
40
20
0
%
control
da
da:da
sc
NRE^TSFO
Dl Pros DNA
Dl Pros PH3
NRE^TS-FO (7DAI)
F > sc
F'
G
NRE^TS-FO > GFP + sc guts
GFP⁻ Dl⁺ cells
GFP⁺ Dl⁺ cells
5
0
5
% of PH3⁺ cells
H
Dl expression (ISC/EBs)
log-counts/cell
4
2
0
sc⁻ve
sc⁺ve

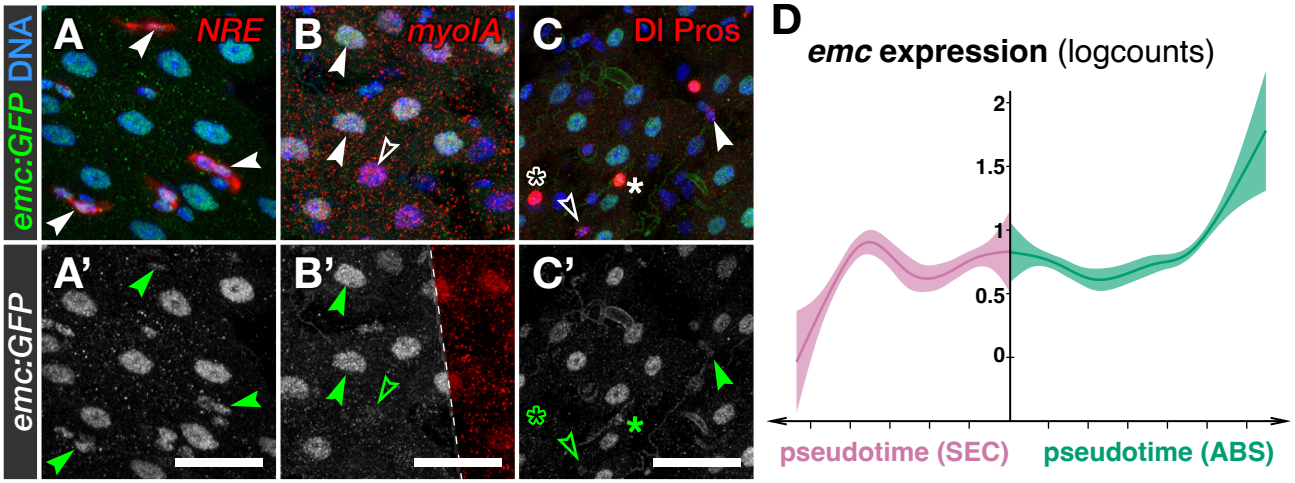
emc:GFP DNA
A NRE
B myoIA
C Dl Pros
emc:GFP
A'
B'
C'
D
emc expression (logcounts)
2
1.5
1
0.5
0
pseudotime (SEC)
pseudotime (ABS)

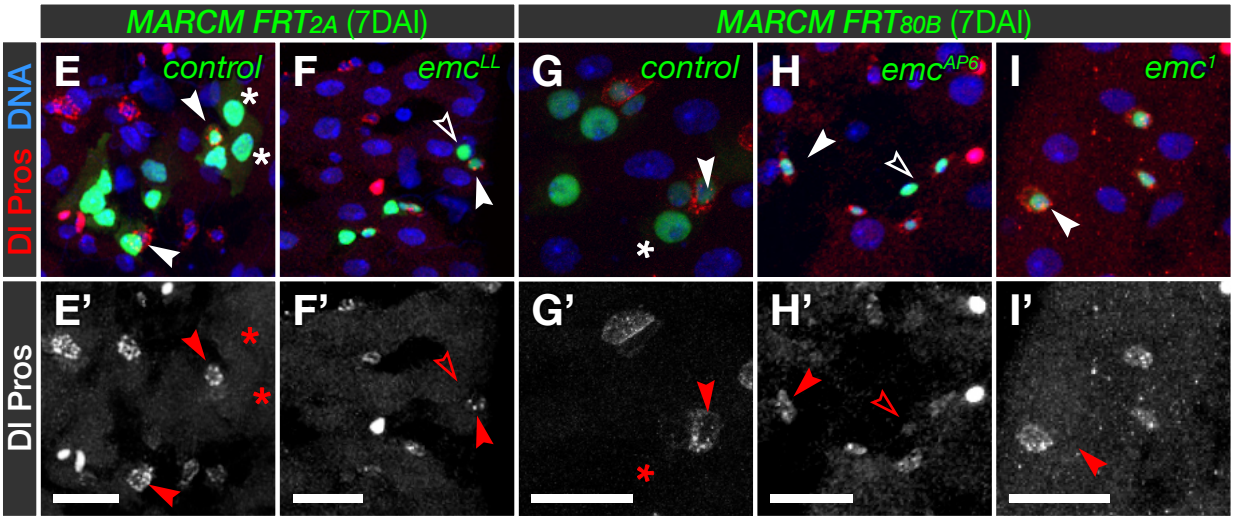
MARCM FRT2A (7DAI)
MARCM FRT80B (7DAI)
Dl Pros DNA
E control
F emcLL
G control
H emcAP6
I emc1
Dl Pros
E'
F'
G'
H'
I'

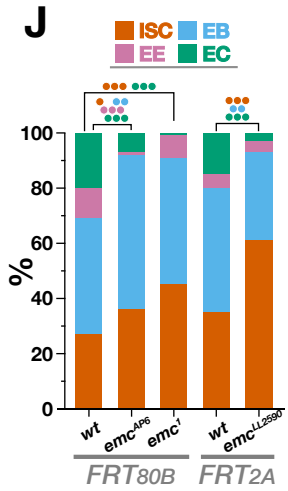
J
ISC
EB
EE
EC
100
80
60
40
20
0
%
wt
emcAP6
emc1
wt
emcLL2590
FRT80B
FRT2A

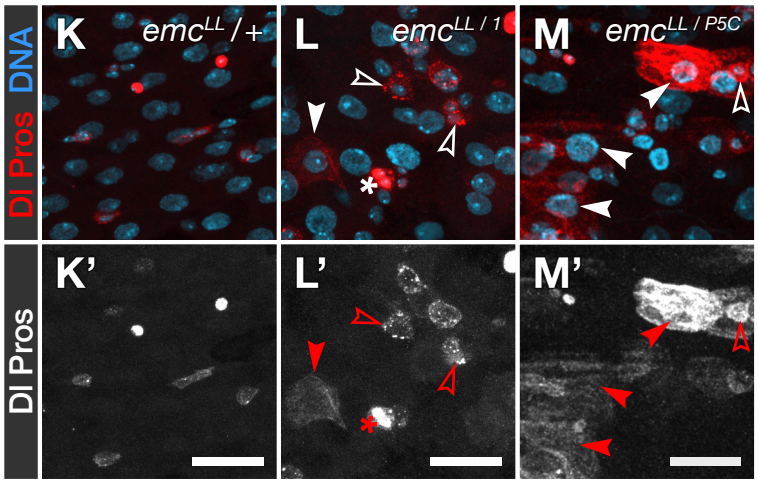
Dl Pros DNA
K emcLL /+
L emcLL / 1
M emcLL / P5C
Dl Pros
K'
L'
M'

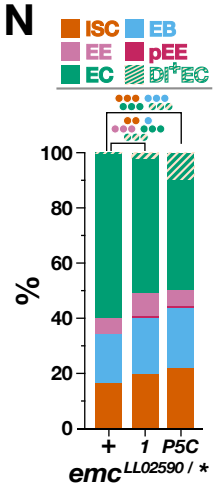
N
ISC
EB
EE
pEE
EC
Dl+EC
100
80
60
40
20
0
%
+
1
P5C
emcLL02590 / *

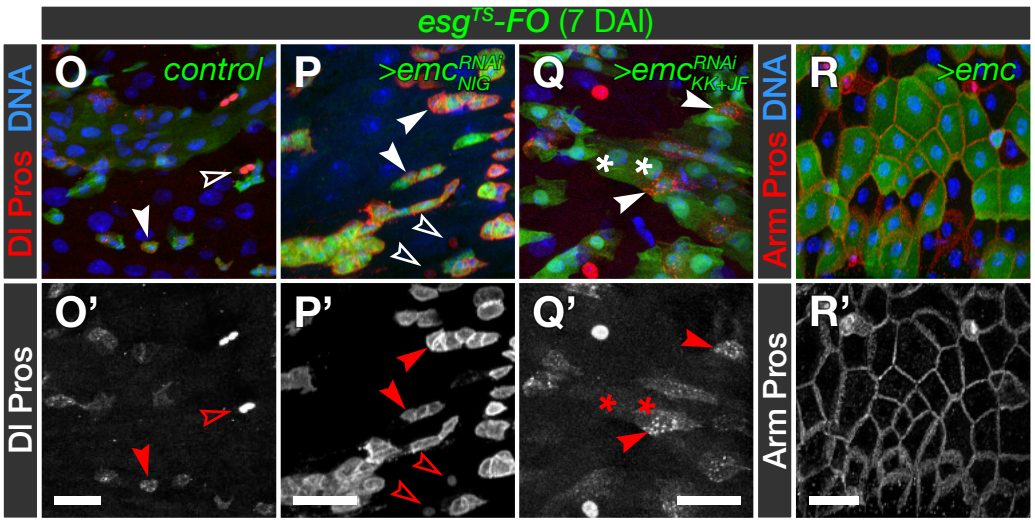
esgTS-FO (7 DAI)
Dl Pros DNA
O control
P >emcRNAi NIG
Q >emcRNAi KK+JF
Arm Pros DNA
R >emc
Dl Pros
O'
P'
Q'
Arm Pros
R'

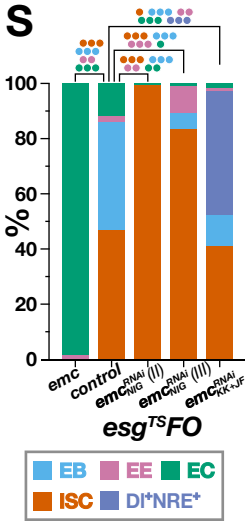
S
100
80
60
40
20
0
%
emc
control
emcRNAi NIG (II)
emcRNAi NIG (III)
emcRNAi KK+JF
esgTSFO
EB
EE
EC
ISC
Dl+NRE+

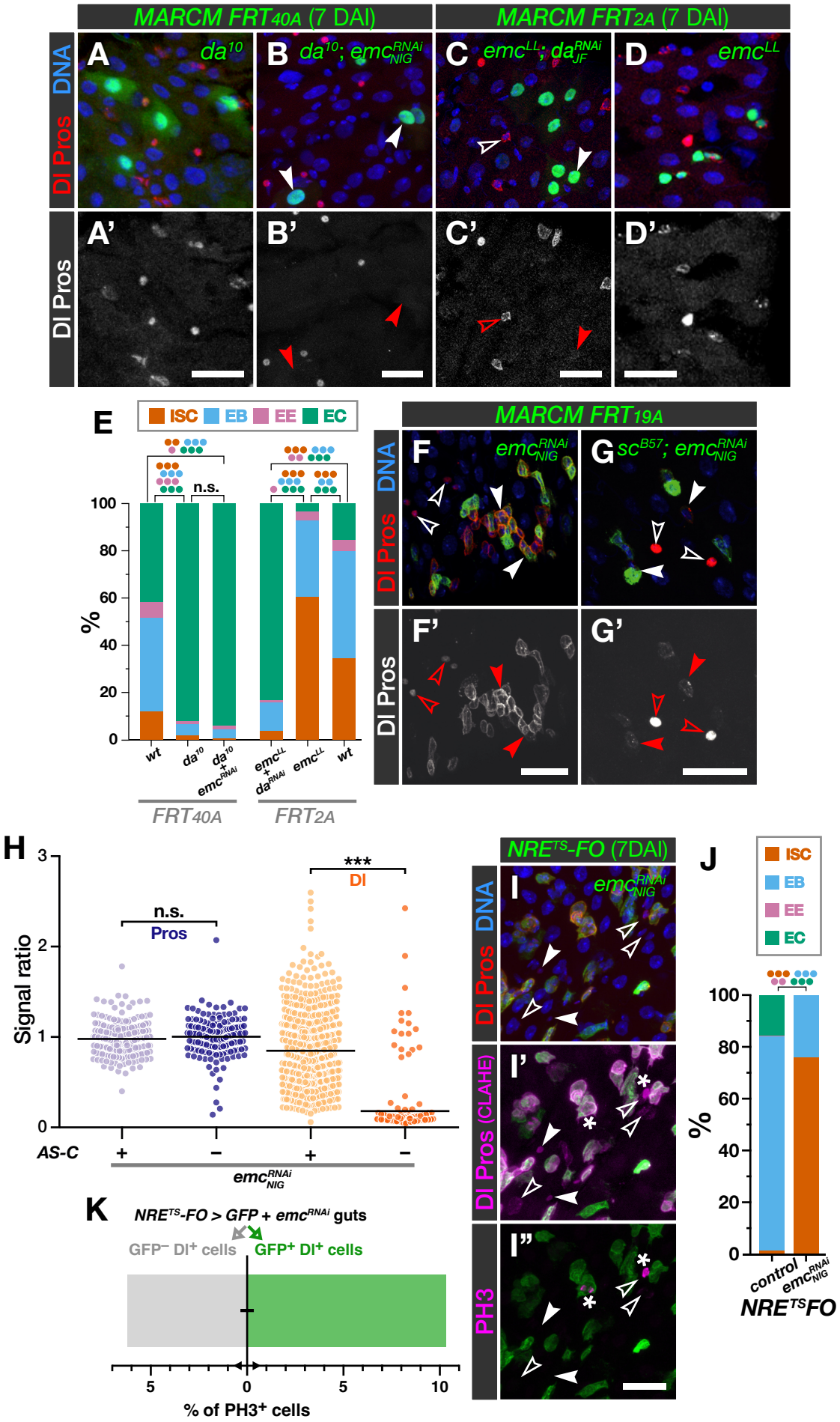
MARCM FRT40A (7 DAI)
MARCM FRT2A (7 DAI)
DNA
Dl Pros
A da10
B da10; emcRNAi NIG
C emcLL; daRNAi JF
D emcLL
A'
B'
C'
D'
E
ISC EB EE EC
n.s.
%
wt
da10
da10 + emcRNAi
emcLL + daRNAi
emcLL
wt
FRT40A
FRT2A
MARCM FRT19A
F emcRNAi NIG
G scB57; emcRNAi NIG
F'
G'
H
Signal ratio
n.s.
Pros
***
Dl
AS-C
emcRNAi NIG
NRETS-FO (7DAI)
I emcRNAi NIG
I'
I''
Dl Pros (CLAHE)
PH3
J
ISC
EB
EE
EC
control
emcRNAi NIG
NRETSFO
K
NRETS-FO > GFP + emcRNAi guts
GFP− Dl+ cells
GFP+ Dl+ cells
% of PH3+ cells

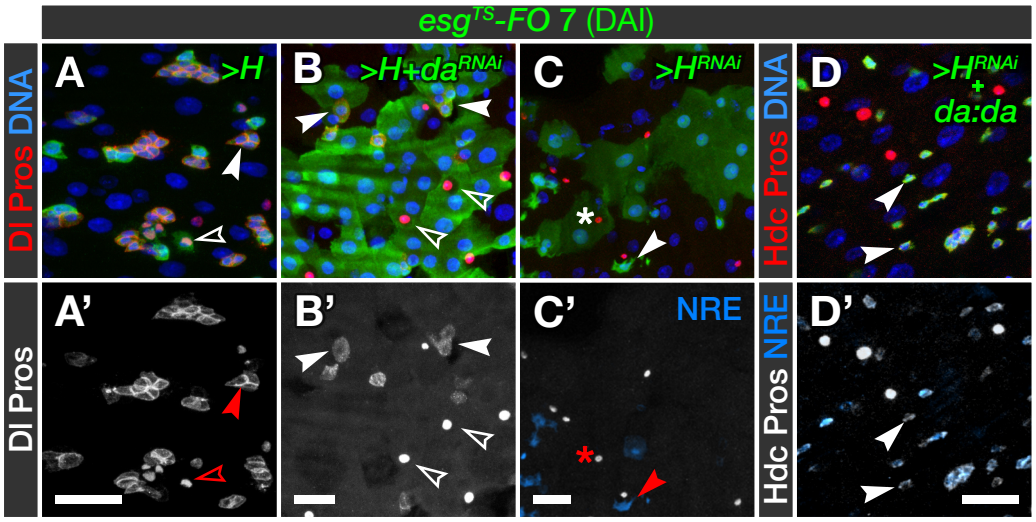
esgTS-FO 7 (DAI)
Dl Pros DNA
A >H
B >H+daRNAi
C >HRNAi
Hdc Pros DNA
D >HRNAi + da:da
Dl Pros
A'
B'
C' NRE
Hdc Pros NRE
D'

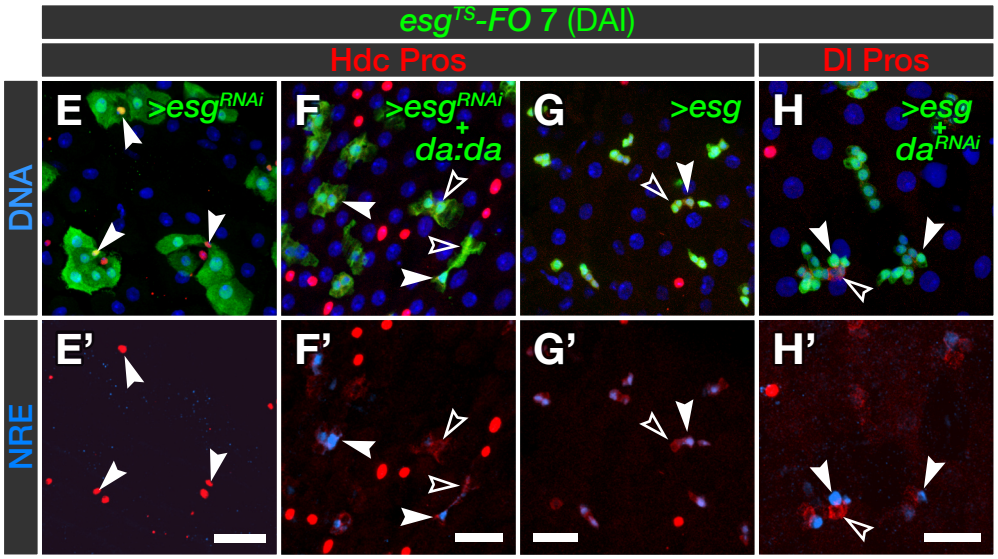
esgTS-FO 7 (DAI)
Hdc Pros
Dl Pros
DNA
E >esgRNAi
F >esgRNAi + da:da
G >esg
H >esg + daRNAi
NRE
E'
F'
G'
H'

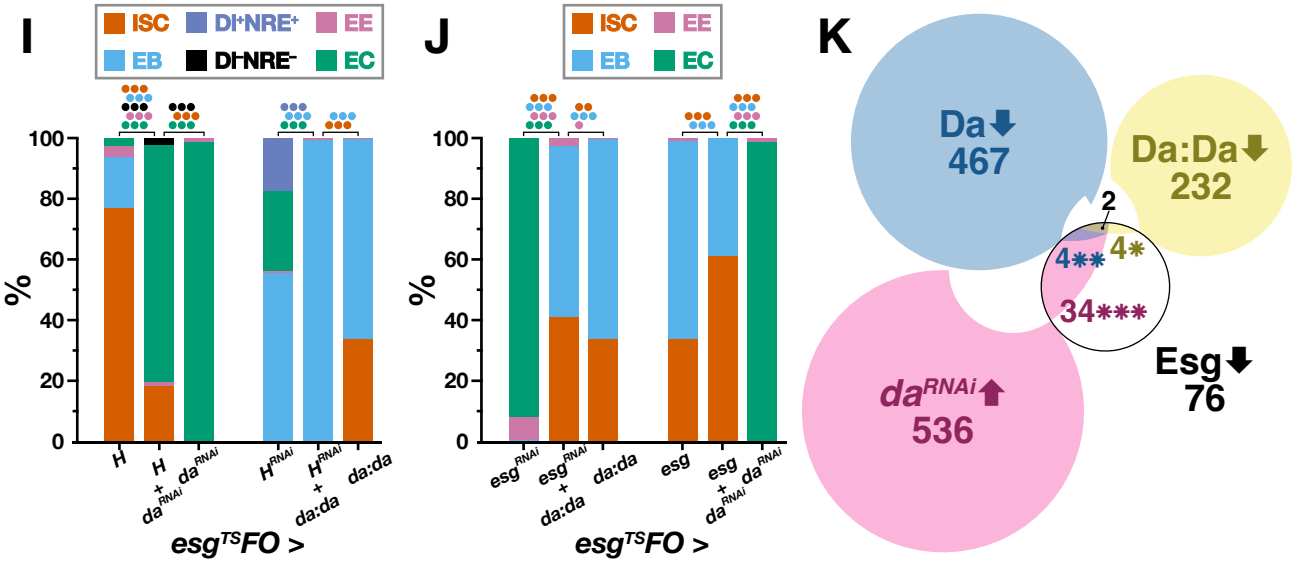
I
ISC
Dl+NRE+
EE
EB
Dl-NRE-
EC
%
H
H + daRNAi
daRNAi
HRNAi
HRNAi + da:da
da:da
esgTSFO >
J
esgRNAi
esgRNAi + da:da
da:da
esg
esg + daRNAi
K
Da⬇ 467
Da:Da⬇ 232
2
4**
4*
34***
daRNAi⬆ 536
Esg⬇ 76